Systematic characterization of cell competition between cancer cells and hepatocytes

An undergraduate thesis presented
by
Andrea Spinazzola, MD

Faculty of Science
Universidad Autónoma de Madrid

PhD course in Biology

Supervisor: Eduardo Moreno

Internal advisor: Carlos García de la Vega

Date of submission: June 6th, 2022

ABSTRACT

Competitive interactions between tumor cells and surrounding healthy cells are constantly present during the progression of a solid tumor, and their outcome has been proposed to affect the growth pattern and clinical behavior. Previous studies have described various mechanistic and molecular aspects that characterize this process, overall indicating that cancer cells behave as supercompetitors, which eliminate neighboring healthy cells to gain vital space for growth and infiltrate the tissue. Nevertheless, there is a lack of systematic characterization of these competitive interactions, particularly in the context of mammalian tumors. In this thesis, I study the competition between numerous cancer cell lines and hepatocytes, and provide a broad characterization of this process in different relevant scenarios, including cells growing *in vitro* in 2D and 3D, and liver metastases. Results show that *in vitro*, only a subset of cancer cell lines are coherently strong or moderate competitors, while the remaining behave as poor competitors. This competitive proficiency predicts the phenotype of liver metastases, with the three strongest competitors generating aggressive metastases with an infiltrative growth pattern. On the contrary, four out of five of the remaining cell lines resulted in a milder disease which often displayed expansile growth. Finally, the competitive phenotype can vary depending on the experimental growth system that is employed.

RESUMEN

Las interacciones de competición entre las celulas tumorales y las celulas sanas vecinas están permanentemente presentes durante la progresión del tumor sólido, y el resultado de dichas interacciones afecta al patrón de crecimiento y comportamiento clínico del tumor. Estudios previos han descrito varios aspectos moleculares y mecánicos que caracterizan este proceso, en particular los que indican que las células tumorales se comportan como supercompetidores,y logran eliminar las células sanas vecinas para conseguir espacio vital para su crecimiento e infiltración en el tejido. Sin embargo, aun es necesaria la caracterización sistemática de dichas interacciones competitivas, particularmente en el contexto de tumores en mamíferos. En esta tesis se ha estudiado la competición entre numerosas lineas celulares de tumores y de hepatocitos y se ha logrado una amplia caracterización de este proceso en diferentes escenarios relevantes, incluido el crecimiento de células in vitro en 2D y 3D, y la metástasis en el hígado. Los resultados muestran que, in vitro, sólo una parte de las lineas celulares tumorales actúan coherentemente como competidores fuertes o moderados, mientras que el resto se comportan pobremente como competidores. Esta habilidad competitiva predice el fenotipo de las metástasis en el hígado, con tres de los competidores fuertes que generan metástasis agresivas y con un patrón de crecimiento infiltrativo. Por el contrario, cuatro de las cinco lineas celulares restantes se obtuvo un patrón mucho más suave de la enfermedad, que,

frecuentemente, mostraba un fenotípo de crecimiento expansivo. Por último, el fenotipo competitivo puede variar en función del sistema de crecimiento experimental que se emplee.

ACKNOWLEDGMENTS

I would like to thank Eduardo Moreno for allowing me to pursue this exciting line of research in his lab, in an autonomous and unconditioned way. During the years of my doctorate, he always showed me respect and trust, and he never made me lack his support for the implementation of this work.

I also want to thank Prof. Carlos de la Vega and Luis Bolaños, from the Autonomous University of Madrid, for their kindness and availability in helping me to deal with different issues related to my PhD program.

A special thank goes to Tania Carvalho, a veterinary pathologist at Champalimaud Foundation, for her wonderful work in evaluating and describing the histopathology of liver metastases.

I would like to thank former and current members of Moreno Lab, including Catarina senior, “los chiquitos” Andres and Mariana, Rato, Ines, Denise, Maria, Dina, Miguel, Pedrinho, Catarina junior, Marta, and Carolina. Their insights were essential to the quality of this thesis.

At last, I want to thank for their precious support the wonderful people who work in the different facilities at Champalimaud Foundation, including Davide and Anna from the Advanced BioImaging and BioOptics Experimental Platform; Ana, Renato and Andre from the Flow Cytometry Platform; Raquel and Ana from the Molecular and Transgenic Tools Platform; Dolores, Isabel and Leonor from the Rodent

Platform; Susana, Sergio and Ines from the Histopathology Platform; Maria and Patrick from the Glasswash and Media Preparation Platform. Their contribution has been essential for the realization of this thesis.

TABLE OF CONTENTS

ABSTRACT i

RESUMEN ii

ACKNOWLEDGMENTS iv

INTRODUCTION 4

1.1 Paradigms of cell competition 5

1.2 Cell competition and cancer 11

1.3 Thesis goals 17

INTRODUCCIÓN 19

RESULTS 22

3.1 Caspase activity is not required for tumor replacement of liver parenchyma 22

3.2 Cancer cells establish different competitive phenotypes with hepatocytes in 2D culture 24

3.3 Cancer cells compress and displace AML12 cells 28

3.4 Growing cells as spheroids alters the competitive behavior of some cancer cells compared to 2D culture 32

3.5 The competitive phenotype of cancer cells *in vitro* correlates with the behavior of liver metastasis 36

3.6 Molecular analysis 39

3.7 Mechanistic analysis 42

3.8 Cell cannibalism plays a minor role in the outcompetition of hepatocytes ...47

3.9 When the space is limited, the growth of poor competitor cancer cells is physically restrained by AML12 cells 49

DISCUSSION 52

CONCLUSIONES 56

MATERIALS AND METHODS 59

6.1 Cell lines. 59

6.2 Drugs. 59

6.3 Generation of MSCV-FasL retroviral vector. 59

6.4 Generation of cells expressing EGFP or TdTomato. 60

6.5 Generation of cells overexpressing FasL. 60

6.6 Cell competition assay in 2D. 61

6.7 Cell competition assay in 3D. 61

6.8 Proliferation analysis. 62

6.9 Conditioned medium experiment. 62

6.10 Supernatant from competing cells. 62

6.11 Phalloidin staining. 63

6.12 Annexin V assay. 63

6.13 Cell cycle analysis. 64

6.14 RT-PCR.....65

6.15 Immunohistochemistry. 66

6.16 Acute liver toxicity. 66

6.17 Experimental liver metastases. 67

6.18 Microscopy imaging and analysis. 67

6.19 Statistical analysis. 68

BIBLIOGRAPHY 69

INTRODUCTION

The destruction of the host tissues and their replacement with tumor are common morphological findings among numerous types of human advanced solid cancer, including both locally advanced primary tumors and metastases [1-4]. In virtue of their physical nature, it is intuitive that solid tumors located within a solid organ need to gain vital space to grow. This may be accomplished by exploiting two different growth patterns: expansive growth and infiltrative growth. Expansive growth is typical of benign tumors and hyperplastic lesions, which compress the surrounding tissues with normally no sign of erosion or infiltration within them. Infiltrative growth characterizes malignant tumors, and results in the destruction of neighboring healthy tissues and their replacement with cancer [2]. Hence, contrary to what happens in benign tumors, cells belonging to different types of solid cancer may develop skills that enable them to infiltrate host tissues. To explain this phenomenon, it has been proposed that cancer cells behave as supercompetitors, which eliminate and replace surrounding healthy cells through a process called cell competition [5-12]. In this thesis chapter, I review the known principles of cell competition, with a focus on the main molecular mechanisms that have been discovered to mediate the process. I also describe how cell competition is exploited in different ways by tumor cells to gain a competitive advantage over healthy cells, which in turn enables tumor development and progression. Finally, I highlight the

limitations of currently available studies in the field, and explain why the research line that has been implemented for the realization of this thesis brings both novelty and relevance.

1.1 Paradigms of cell competition

Cell competition is a widespread phenomenon, conserved across species, in which cells sense their fitness status, and the confrontation of cells with different fitness levels drives the elimination of those cells (named as loser) that are less fit than their neighbors (named as winner) [FIG. 1]. First discovered in the developing wing imaginal disc of *Drosophila melanogaster* in 1975 [37], cell competition is now known to occur not only in growing tissues, but also in adult tissues, in post-mitotic cells, and in the nervous system [14,15,36]. Cell selection and fitness comparison are essential to numerous biological processes of the organism, including but not limited to the correction of developmental errors, the preservation of adult tissue health, and the physiopathology of tumors [14,15,36].

Fitness comparison and cell selection are executed through different mechanisms, which include the competition for a limiting amount of extracellular survival factors, the generation of mechanical stress, the direct stimulation of death receptors, and the expression of specific fitness fingerprints [FIG. 2] [31]. As a consequence of these processes, the elimination of loser cells is accomplished by various means, such as

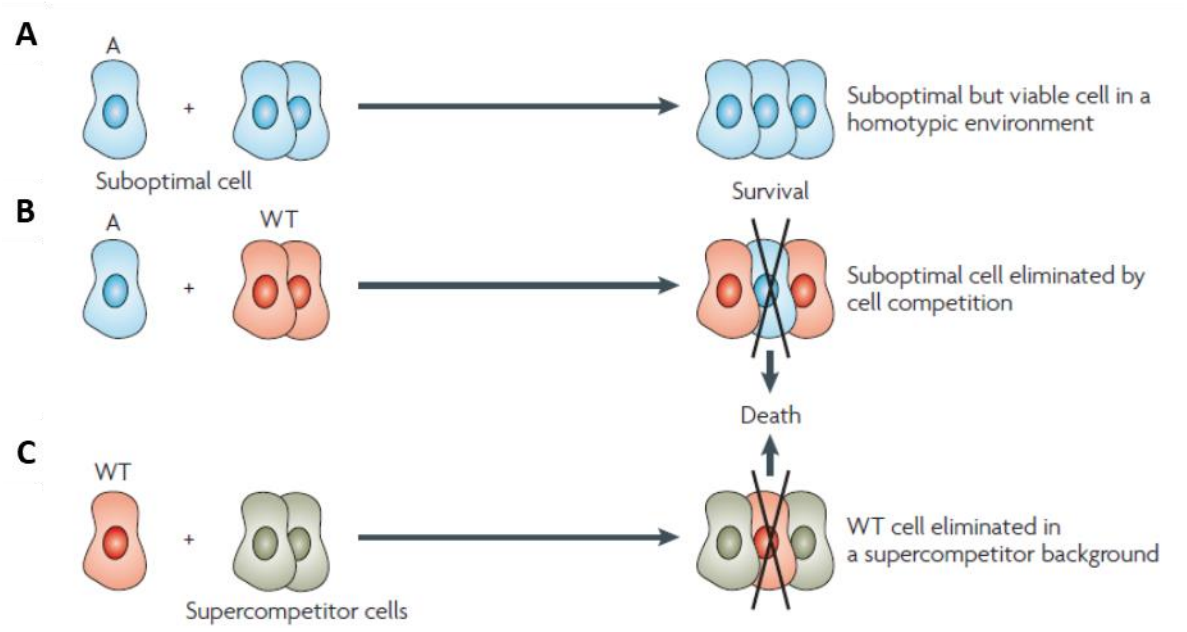

Fig. 1: Definition of cell competition. (Adapted from Moreno, 2008; ref. 5) **(A)** During cell competition, cells that are suboptimal, for example due to a mutant genotype A, are viable when situated in a homotypic environment. **(B)** Suboptimal cells are eliminated when they confront with their fitter counterparts, for example wild type (WT) cells. **(C)** Supercompetitor cells have mutations that increase their fitness status, and are able to eliminate surrounding WT cells and colonize the tissue.

induction of apoptosis [7-9,33], apical extrusion [23,24,34], induction of necroptosis [29], and entosis (or cell cannibalism) [78,79].

During the competition for survival factors, winner cells are those with a higher ability to capture the survival signals compared to loser cells. A notable example is the competition for the morphogenetic factor decapentaplegic (Dpp) in the wing imaginal disc of *Drosophila*, which leads to the elimination of cell clones that have deleterious mutations in ribosomal proteins when confronted with wild type (WT)

cells [42] [FIG. 2A]. Similarly, the ability to transduce IL-7 signals regulates the turnover of T-cell progenitors in the mouse thymus, and selects young T-cell progenitors at the expense of old progenitors [43].

Mechanical cell competition takes place within an environment where the total available space is restricted, and the homeostatic mechanisms that control cell density and tissue proliferation are eluded by clones of cells that overproliferate and promote tissue crowding. This in turn results in the generation of mechanical forces across the tissue, which are particularly intense at the interface between cell populations with different growth rates. The differential sensitivities to mechanical forces result in the elimination of cells that are hypersensitive to mechanical stress (losers) and the compensatory gain of winners to the tissue space [45] [FIG. 2B]. For example, in the *Drosophila* notum, clones of cells harboring activating RasV12 mutations overproliferate, and promote tissue compaction due to overcrowding. This causes the downregulation of epidermal growth factor (EGF)/extracellular-regulated kinase (ERK) signaling in WT cells, which drives their elimination via apoptosis followed by delamination [9,47]. In the canine kidney cell line MDCK, the knockdown (KD) of the apico-basal polarity gene *Scribble* ($Scrib^{KD}$) causes hypersensitivity to compaction upon culture with WT MDCK cells. In such conditions, $Scrib^{KD}$ clones upregulate p53 in a Rho-associated kinase (ROCK) and

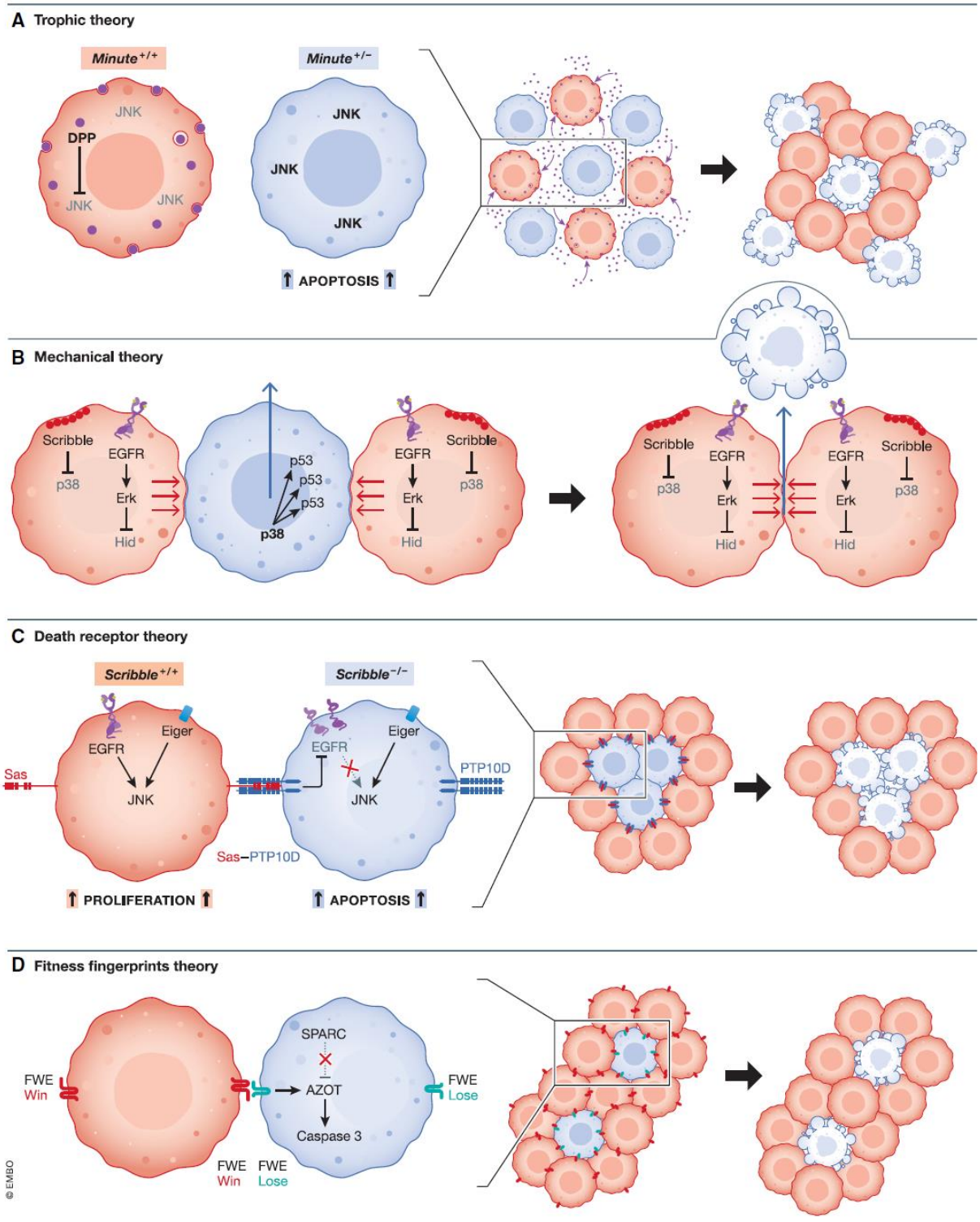
A Trophic theory
Minute+/+
JNK
DPP
JNK
JNK
Minute+/−
JNK
JNK
JNK
APOPTOSIS
B Mechanical theory
Scribble
EGFR
p38
Erk
Hid
p53
p53
p53
p38
C Death receptor theory
Scribble+/+
Eiger
EGFR
JNK
Sas
Scribble−/−
Eiger
EGFR
JNK
PTP10D
Sas–PTP10D
PROLIFERATION
APOPTOSIS
D Fitness fingerprints theory
FWE
Win
SPARC
AZOT
Caspase 3
FWE
Lose
FWE
Win
FWE
Lose
© EMBO

Fig. 2: Mechanisms of cell competition. (Adapted from Parker at al, 2021; ref. 31) **(A)** During competition for trophic factors, winner cells are those with a higher ability to capture a limiting amount of extracellular survival signal compared to loser cells. For example, the so called Minute cells have deleterious mutations in genes encoding ribosomal proteins, and are outcompeted by neighboring wild-type (WT) cells based on their reduced ability to capture the morphogen Dpp. **(B)** Mechanical cell competition arises due to the confrontation of cells with differential sensitivities to mechanical forces. When the available space is restricted, clones of cells that overproliferate lead to tissue crowding. This leads to high levels of mechanical stress and deformation across the tissue, resulting in the elimination of loser cells, for example via the upregulation of the apoptotic proteins p38, p53, and Hid. **(C)** Death receptors are membrane proteins that are ubiquitously expressed in the body. Healthy cells can induce the elimination of suboptimal mutant neighbors, such as clones with deleterious mutations in Scribble, by expressing cell surface death ligands and directly activating death receptors on mutant cells. **(D)** Neighboring cells compare their fitness status through the expression of different isoforms of the transmembrane protein Flower (Fwe), which act as fitness fingerprints. The confrontation of cells expressing low-fitness isoforms (Fwe^{Lose}) with cells expressing high-fitness isoforms (Fwe^{Win}) results in the upregulation of Azot in loser cells, which induces caspase-dependent apoptosis.

stress kinase p38 dependent manner, which leads to apoptosis and extrusion from the cell monolayer [33].

Death receptors are cell membrane proteins that belong to the tumor necrosis factor (TNF) receptor superfamily, which in mammalian cells includes TNF receptors, Fas receptor, and TNF-related apoptosis-inducing ligand (TRAIL) receptors. Upon binding of the cognate ligands, death receptors initiate a cytotoxic signaling cascade which culminates in the activation of effector caspases and apoptotic cell death [27].

Some forms of cell competition take place when different circumstances lead some cells to express death ligands, at the cell membrane or as secreted molecules, which activate death receptors either in an autocrine manner or in bystander cells [FIG. 2C]. For example, in the wing imaginal disk of *Drosophila*, when polarity deficient epithelial cells ($Scrib^{KD}$) come in contact with WT cells, they are eliminated from the developing epithelia. This process has been reported to depend upon different molecular mechanisms, which include the expression of Eiger, the *Drosophila* TNF homolog, and downstream JNK activation in loser cells [48], as well as the lateral re-localization of ligand stranded at second (Sas) on WT cells and the surface receptor PTP10D on Scribble mutants. This results in the transactivation of Sas-PTP10D signaling and the elimination of the polarity-defective cells [49].

Fitness fingerprints are molecules that are located at the cell membrane and inform neighboring cells of the cellular fitness status through direct contact between cells. The confrontation of cells expressing low-fitness fingerprints with cells expressing high-fitness fingerprints results in the elimination of the loser cells [FIG. 2D]. To date, the most characterized and experimentally validated fitness fingerprint is Flower (Fwe), a transmembrane protein that is expressed in different win (Fwe^{Win}) or lose (Fwe^{Lose}) isoforms according to a cell's fitness status, and whose role as cell fitness indicator is conserved across *Drosophila* [38], mouse [11], and human [10]. Importantly, membrane Fwe^{Lose} presence does not autonomously induce apoptosis,

since Fwe^{Lose} cells are not eliminated when surrounded by Fwe^{Lose} neighbors. A relative difference in Fwe levels between cells is sufficient to trigger apoptosis of cells with a higher Fwe^{Lose} expression or in cells with lesser expression levels of Fwe^{Win}, independently of their actual fitness status [10,11,38]. In *Drosophila* it has been shown that, when cell clones compete through Fwe fitness fingerprints, loser cells upregulate the expression of Azot, which in turn is required for their elimination [50]. The Fwe code and its downstream mediator Azot appear to be common, tunable read-out of cellular fitness, particularly in *Drosophila*, where they mediate the competitive interactions that are induced by various triggers, such as a mutation in genes encoding ribosomal proteins, deleterious mutations in apico-basal polarity genes, and differential expression of dMyc [38,50].

1.2 Cell competition and cancer

Competitive interactions between transformed cells and the surrounding host cells are constantly present during all phases of cancer development and progression, from the appearance of pre-tumoral cells to the establishment of a primary tumor and the subsequent development of metastases [5,13,31]. The outcome of these interactions has been shown to be relevant in determining various aspects of the disease, including the morphology of tumor lesions, the clinical behavior, and the response to anticancer therapy. Although cell competition acts as a tumor-

suppressive mechanism during the early stages of carcinogenesis [24,29,34,35,45], cancer cells can rewire this process to foster their growth and dissemination throughout the organism [5-10,13]. Indeed, some genetic alterations that are commonly found in human cancers, such as increased expression of Myc [12,26], activation of the WNT signaling pathway [39-41], or constitutive signal through EGF receptor [8], lead to an increase of fitness, and generate supercompetitor cells which can eliminate neighboring WT cells and invade the tissue. Accordingly, it has been proposed that supercompetition may promote tumor progression by fostering the elimination and replacement of healthy cells by pretumoral cells and cancerous cells [5,31].

Available literature shows that cancer cells can exploit various forms of cell competition to outcompete surrounding healthy cells. Among these, the competition for trophic factors seems to play a minor role compared to the others. Nevertheless, a recent study found that, in leptomeningeal metastases, cancer cells compete with macrophages for the limited supply of iron that is present in the cerebrospinal fluid. To win the clash, cancer cells upregulate the high affinity iron-capturing system constituted by the iron-binding protein lipocalin-2 (LCN2) and its receptor SCL22A17, and outcompete macrophages by limiting their iron supply, potentially escaping immune attack [FIG. 3A] [44].

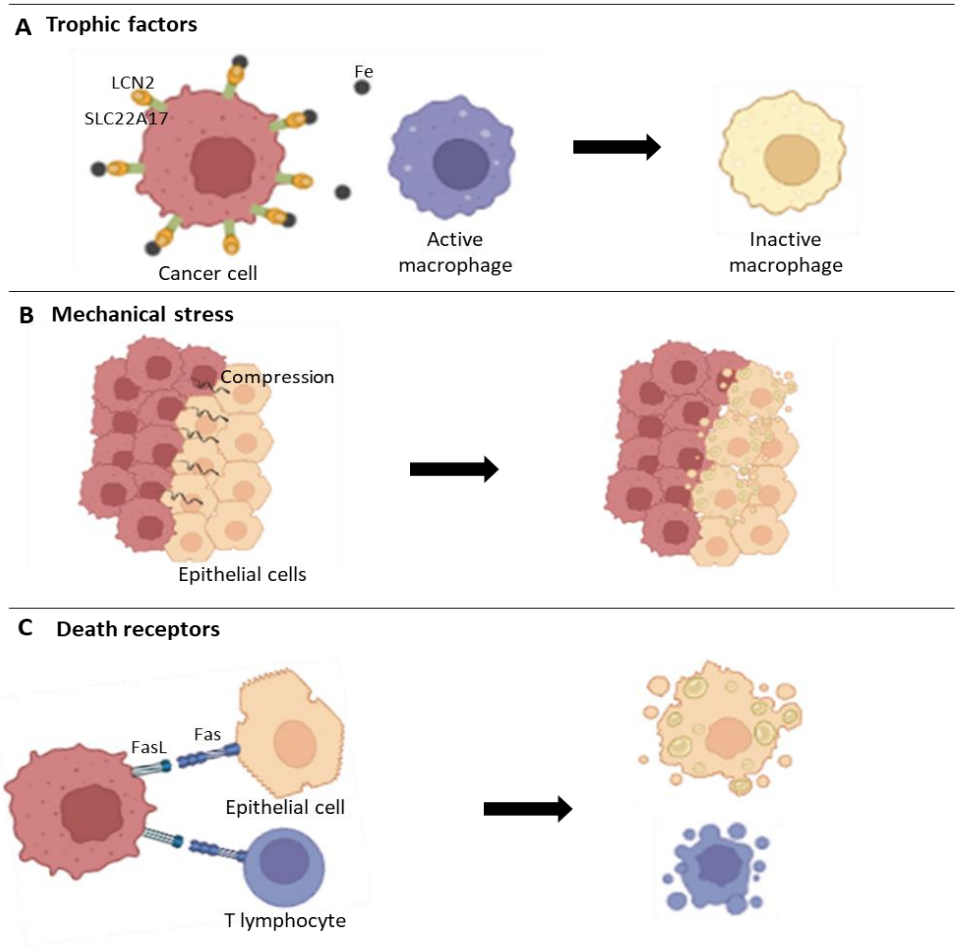
A Trophic factors
LCN2
SLC22A17
Fe
Cancer cell
Active macrophage
Inactive macrophage
B Mechanical stress
Compression
Epithelial cells
C Death receptors
FasL
Fas
Epithelial cell
T lymphocyte
D Fitness fingerprints
Fwe Win
Fwe Lose
E Cell cannibalism
Phagocytic engulfment
Lysosomal membrane

Fig. 3: Cell competition and cancer. **(A)** In leptomeningeal metastases, cancer cells upregulate the iron-capturing system LCN2/SCL22A17, and outcompete macrophages by depriving their iron supply. This induces a functional inactivation of macrophages, thus enabling tumor immune evasion. **(B)** Cancer cells are less sensitive to compaction compared to healthy cells. This allows them to keep proliferating and expand within tissues that are already occupied by healthy cells and that are subjected to space constraints. The resulting mechanical stress allows cancer cells to compress and eliminate neighboring healthy cells. **(C)** The upregulation of membrane Fas ligand (FasL) enables tumor cells to directly induce apoptosis in neighboring healthy cells which express Fas receptor. This may generate vital space for growth by eliminating parenchymal cells at the tumor border. It may also promote the suppression of antitumor immunity by counterattacking tumor-infiltrating immune cells. **(D)** Cancer cells increase the expression of Fwe^{Win} isoforms compared to the adjacent healthy cells, which often express Fwe^{Lose} isoforms. In doing so, cancer cells exploit Fwe-mediated cell competition to gain a competitive advantage over neighboring stromal cells. **(E)** Cell cannibalism involves the phagocytosis of healthy cells (e.g. immune cells) by tumor cells, which is followed by their lysosomal digestion.

Mechanical cell competition is predicted to have a strong impact on the initiation and the progression of cancer [80]. Increased homeostatic pressure has been proposed to be a characteristic trait of solid tumors, due to their uncontrolled growth within tissues that are subjected to space constraints [81]. Although direct evidence *in vivo* in mammalian tumors is still lacking, available data suggest that cancer cells are less sensitive to compaction compared to the surrounding host cells. This sustains their ability to keep proliferating and expanding by allowing tumor cells to eliminate neighboring healthy cells, upon compression, and infiltrate the tissue [FIG. 3B] [77].

During the past four decades, numerous studies have investigated the biological relevance of death ligands expression by tumor cells, with the majority of them focusing on Fas ligand (FasL). The overall evidence from these studies indicates that FasL may function as a tumor-promoting tool, enabling cancer cells to outcompete the surrounding host cells that express Fas receptor by directly inducing apoptosis [FIG. 3C] [16-21]. The analysis of human specimens revealed that tumor cells often upregulate the expression of FasL, and this was evident among numerous histological types, such as colon cancer [16,17], breast cancer [18,57], retinoblastoma [51], gastric adenocarcinoma [20,52,53], pancreatic carcinoma [21,67], and others [54-56,58]. Interestingly, some studies found that, within a tumor lesion, FasL is more expressed at the advancing border, that is in the area of tumor invasion within hot tissues [21,59]. The expression of FasL has been positively correlated with different clinical features of the disease. For example, it has been implicated in the pathogenesis of breast cancer [18,59] and ovarian cancer [60], in the adenoma-carcinoma progression during colon carcinogenesis [61-63], and in the development of cutaneous squamous cell carcinoma [64]. Moreover, the expression of FasL has been shown to associate with a more advanced disease stage as well as to independently predict a worse prognosis compared to no expression in patients with breast cancer [18,57], colon cancer [65,66], pancreatic carcinoma [21,67], ovarian cancer [60], hepatocellular carcinoma [68], and cervical cancer [69,70].

Experiments in murine models have confirmed that, besides pursuing the generation of vital space for growth, by eliminating parenchymal cells at the tumor border [16,19], the expression of death ligands may enable cancer cells to counterattack and kill immune cells, thus suppressing antitumor immunity [71-74].

To date, the only available evidence of Fwe-mediated cell competition in mammalian tumors comes from two studies from the lab of Eduardo Moreno. The first study characterized mouse Fwe isoforms in a model of skin papilloma development upon exposure to the carcinogens 7,12-dimethylbenz[α]anthracene (DMBA) and 12-O-tetradecanoylphorbol-13-acetate (TPA). The expression of one Fwe^{Lose} isoform was significantly increased in the papilloma-surrounding tissue compared to the skin of control mice [11]. Importantly, the knock-out of the Fwe gene in mice conferred protection against skin carcinogenesis, resulting in a significantly lower number of papillomas upon exposure to DMBA/TPA compared to WT mice. In the second study, the authors demonstrate that human cancer cells increase the expression of Fwe^{Win} isoforms compared to the adjacent healthy cells, and exploit Fwe-mediated cell competition to gain a competitive advantage over neighboring stromal cells, which often express Fwe^{Lose} isoforms [FIG. 3D] [10]. In xenograft mouse models, the inhibition of the expression of Fwe proteins in human cancer cells was sufficient to reduce tumor growth and metastasis, and increased the sensitivity to chemotherapy.

At last, it has been reported that cancer cells may outcompete normal cells by engulfing and digesting them, in a process called cell cannibalism [FIG. 3E] [22]. In human specimens, tumor cell cannibalism has been mostly observed towards immune cells rather than parenchymal cells. The outcompetition of healthy cells through this process may serve as a tool to feed aggressive cancer cells, particularly under starvation conditions.

1.3 Thesis goals

The studies that I reviewed show that tumor cells can exploit different competitive mechanisms to eliminate and replace neighboring healthy cells and infiltrate host tissues. This allows solid cancers to keep on growing within an environment that is already occupied by healthy cells and that is subjected to space limitations. Although some data are available describing the molecular mechanisms and the biological relevance of tumor supercompetition, there is a deep lack of knowledge about different essential features, including a broad phenotypic and mechanistic characterization in mammalian tumors. In fact, one limitation of the studies that I reviewed is that they evaluated only one or a few tumor models. Furthermore, most of them have been conducted focusing only on one single mechanism of cell competition. Accordingly, a systematic analysis of the competitive interactions

between cancer cells and healthy cells, adopting numerous tumor models and assessing different forms of cell competition, is strongly needed.

In this thesis, I try to accomplish part of this task by studying the interaction between numerous cancer cell lines, deriving from mouse and human tumors, and mouse hepatocytes. The goal is to provide a phenotypic and mechanistic characterization of this process in different relevant scenarios, including cells growing in two dimensions (2D), cells growing as spheroids in three dimensions (3D), and experimental metastases to the liver. This research explores various forms of cell competition, with the aim to characterize the mechanisms that promote the elimination of hepatocytes during the confrontation with cancer cells. As mentioned above, infiltrative growth is a widespread trait of solid cancers, and relies on the elimination of healthy cells. Accordingly, the comprehensive characterization of tumor supercompetition might lead, in the future, to the development of innovative therapeutic options for patients with advanced solid cancer, such as pharmacological agents that prevent the elimination of healthy cells.

INTRODUCCIÓN

En humanos, tanto la destrucción de tejido del huésped como su reemplazo por células tumorales representan uno de los hallazgos más frecuentes, a nivel morfológico, en los distintos tipos de tumores sólidos, y que incluyen tanto a los tumores avanzados como a las metástasis. De acuerdo con su naturaleza, se asume que los tumores sólidos localizados en un órgano necesitan obtener espacio para poder crecer. Este fenómeno puede presentarse en dos patrones diferentes: crecimiento expansivo y crecimiento infiltrativo. El crecimiento expansivo es típico de los tumores benignos y de lesiones hiperplásicas que comprimen los tejidos circundantes y, normalmente, no va acompañado por ningún signo de erosión o infiltración de dichos tejidos. El crecimiento infiltrativo, característico de los tumores malignos, tiene como resultado la destrucción del tejido sano que lo rodea y su reemplazo por células tumorales. Por lo tanto, contrariamente a lo que sucede en los tumores benignos, las células de tumores malignos pueden desarrollar capacidades que les permiten un crecimiento infiltrativo. Para explicar este fenómeno, se ha propuesto que las células tumorales actúan como supercompetidoras, de manera que eliminan y reemplazan a las células sanas circundantes mediante un proceso llamado competición celular. Los resultados obtenidos hasta la fecha indican que las células tumorales pueden utilizar los mecanismos de competición para promover el crecimiento de tumores sólidos

malignos en un ambiente ya ocupado por células sanas y que disponen de un espacio limitado.

En la bibliografía hay referencias en la que se describen los mecanismos moleculares de la supercompetición tumoral y su relevancia biológica. Sin embargo, aún existe un profundo desconocimiento sobre las características esenciales de dicha supercompetición, incluyendo su caracterización -tanto a nivel fenotípico y funcional - en tumores de mamíferos. De hecho, una de las limitaciones de los estudios realizados previamente, es que en estos solo se evalúan uno o unos pocos modelos tumorales. Es más, estos estudios solo se centran en uno de los mecanismos de la competición celular. En consecuencia, es necesario realizar un análisis sistemático de las interacciones mediante competición entre células tumorales y células sanas, que incluya varios modelos tumorales y que estudie diferentes formas de competición celular.

En esta tesis se aborda parte de esta tarea. Para ello, se ha estudiado la interacción en múltiples líneas celulares tumorales, derivadas de humanos y de ratones, así como en hepatocitos de ratón. El objetivo principal de este trabajo es caracterizar este proceso -de forma fenotípica y funcional- en los diferentes escenarios. Este planteamiento incluye el crecimiento de células en dos dimensiones, en esferoides tridimensionales y en metástasis en el hígado. Esta tesis explora las diferentes formas de competición celular, con la finalidad de caracterizar los mecanismos que

promueven la eliminación de los hepatocitos tras su confrontación con células tumorales. Como se ha mencionado anteriormente, el crecimiento infiltrativo es una característica general presente en tumores malignos sólidos y que se basa en la eliminación de las células sanas. Este trabajo se enmarca, además, en la caracterización exhaustiva del fenómeno de la supercompetición tumoral que, en el futuro, podría conducir al desarrollo de nuevas opciones terapéuticas para pacientes con tumores malignos sólidos como, por ejemplo, agentes farmacológicos que impidan la eliminación de las células sanas.

.

RESULTS

3.1 Caspase activity is not required for tumor replacement of liver parenchyma

Different studies in *Drosophila* and mice have shown that the outcompetition of loser cells is often executed through a caspase-dependent form of cell death. The genetic inhibition of caspases prevented the elimination of loser cells and the expansion of winner clones [7-9,42,76]. Similarly, the activation of Fas receptor generally triggers a caspase-dependent form of cell death, which is called extrinsic apoptotic pathway [27]. Accordingly, we decided to test whether the continuous administration of Emricasan, a highly potent and specific pancaspase inhibitor, may inhibit the growth of liver metastases by preventing the elimination of hepatocytes and other stromal cells. Due to the short half-life of Emricasan [75], we chose to administer it via an ALZET osmotic pump, which was implanted subcutaneously. As a first step, we checked the pharmacological activity of Emricasan over 2 weeks, that is the duration of dispense of the osmotic pumps that we used. In a mouse model of fulminant liver toxicity, due to intravenous injection of the Fas receptor agonistic antibody Jo2, we found that Emricasan was highly efficacious in preventing liver damage at all the time points studied [FIG. 4A-C]. Mice treated with Emricasan showed no sign of toxicity, whereas all control mice appeared moribund 3 hours after the administration of the Jo2 antibody. The livers of control mice were diffusely hemorrhagic, as expected in this model, while those from mice treated with

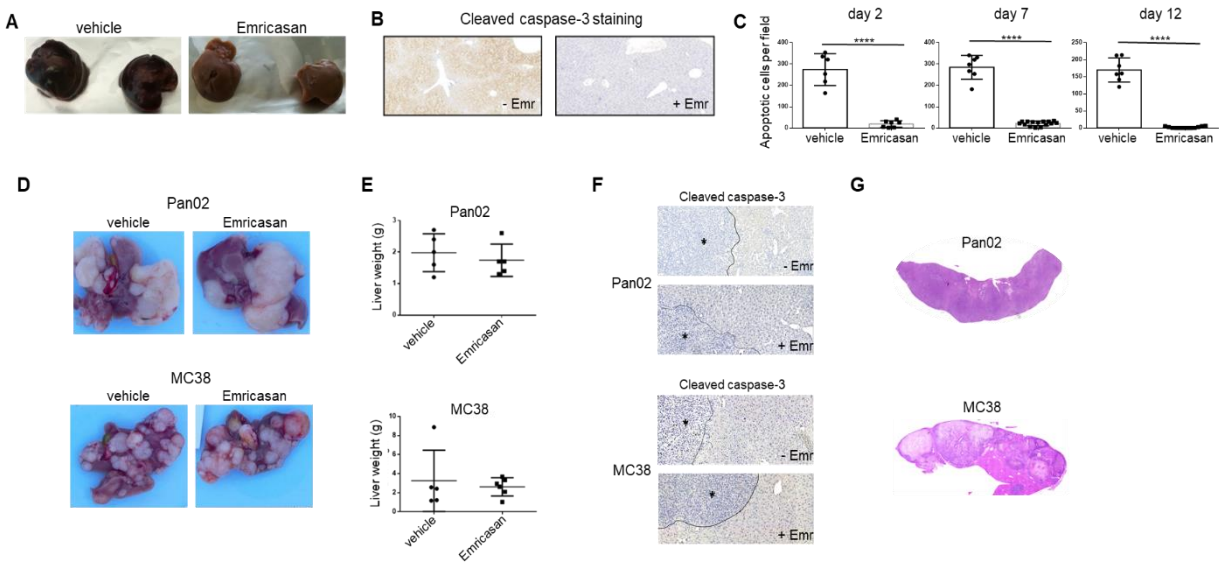

Fig. 4: Caspase inhibition does not affect the growth and the morphology of experimental liver metastases. **(A)** Representative images of livers collected 3 hours after the intravenous injection of a Fas receptor-agonistic antibody in mice receiving Emricasan (15 mg/Kg/day) or vehicle. **(B)** Representative images of liver sections, from **A**, stained with an anti-cleaved caspase-3 (cCasp-3) antibody and counterstained with hematoxylin. **(C)** Quantification of cCasp-3 positive cells form the experiment in **B**. The y axis indicates the number of cells that are positive for cCasp-3 per field of view. **(D)** Representative images of livers collected 30 days after the intrasplenic injection of MC38 cells and Pan02 cells. Mice were treated with Emricasan or vehicle for 27 days. Metastatic foci can be recognized due to their white color. **(E)** Quantification of the metastatic load, expressed by the mean of the weight of livers in each experimental group. This is compared between mice treated with Emricasan and controls for each tumor type. **(F)** Representative images of the tumor-liver interface after staining with an anti-cCasp-3 antibody and counterstained with hematoxylin. Tumor lesions are marked with an asterisk. **(G)** Examples of liver lobes that have been extensively replaced by cancer.

Emricasan appeared normal [Fig. 4A]. After staining of liver sections for cleaved caspase-3 (cCasp3), a marker of apoptosis, we observed massive and diffuse death

of the hepatocytes in control mice, whereas there were few to scant apoptotic cells in mice treated with Emricasan [Fig. 4B-C].

Next, we generated liver metastases by injecting the pancreatic cancer cell line Pan02 and the colon cancer cell line MC38 into the spleen of syngeneic C57BL/6 mice. Three days after the tumor challenge, we implanted the osmotic pumps, and replaced them with new ones after 14 days. Results show no significant difference between experimental animals and controls in terms of metastatic burden and tumor morphology, in either tumor model [FIG. 4D-E]. To our surprise, after staining for cCasp3, positive cells were hardly detectable at the tumor border, independently of the treatment with Emricasan [FIG. 4F]. Although caspases were not active, the liver parenchyma was still being replaced by cancer, especially in mice injected with Pan02 cells [FIG. 4G]. Altogether, these data show that caspase-dependent cell death does not cause the outcompetition of liver cells by metastatic tumor cells.

3.2 Cancer cells establish different competitive phenotypes with hepatocytes in 2D culture

To systematically study the competitive interactions between cancer cells and hepatocytes, which constitute the most abundant cell population in the liver [32], we set up a cell competition assay *in vitro*. We cultured together, in 2D, the murine hepatocyte cell line AML12, expressing EGFP, and numerous cancer cell lines

expressing TdTomato (TdT). Cells were seeded subconfluent, at a ratio AML12 cell-cancer cell of 3:1 for murine tumor cells, and 2:1 for human tumor cells. The culture was continued for 12 days, and was periodically monitored through imaging with a confocal microscope. As a readout for the population size of AML12 cells during the experiment, we quantified the total area per field of view occupied by GFP-labeled cells.

We tested eight murine cancer cell lines, and found that only two of them, namely B16 cells and 4T1 cells, behave as strong competitors, resulting in a substantial (>60%) to total loss of AML12-EGFP cells from the culture [FIG. 5A-C]. In parallel, B16 cells and 4T1 cells colonized the whole culture area within a few days. On the other hand, MC38 cells, Pan02 cells, LLC cells, and CT26 cells lead only to a minimal decrease (≤20%), or even to an increase in the AML12-EGFP population, and did not colonize the whole area of the well. Accordingly, we define these cell lines as “poor competitors”, in the sense that they coexist with AML12 cells without major competitive outcomes. EO771 cells showed a moderate competitive proficiency, with a slow but consistent loss of AML12 cells and the colonization of the majority of the culture area. Finally, Renca cells induced a significant loss of AML12-EGFP cells and colonized around half of the culture area during the first 8 days. This was followed by a stall, without major changes in both cell populations, which lasted until day 20 of culture, when we ended the experiment [FIG. 5A and

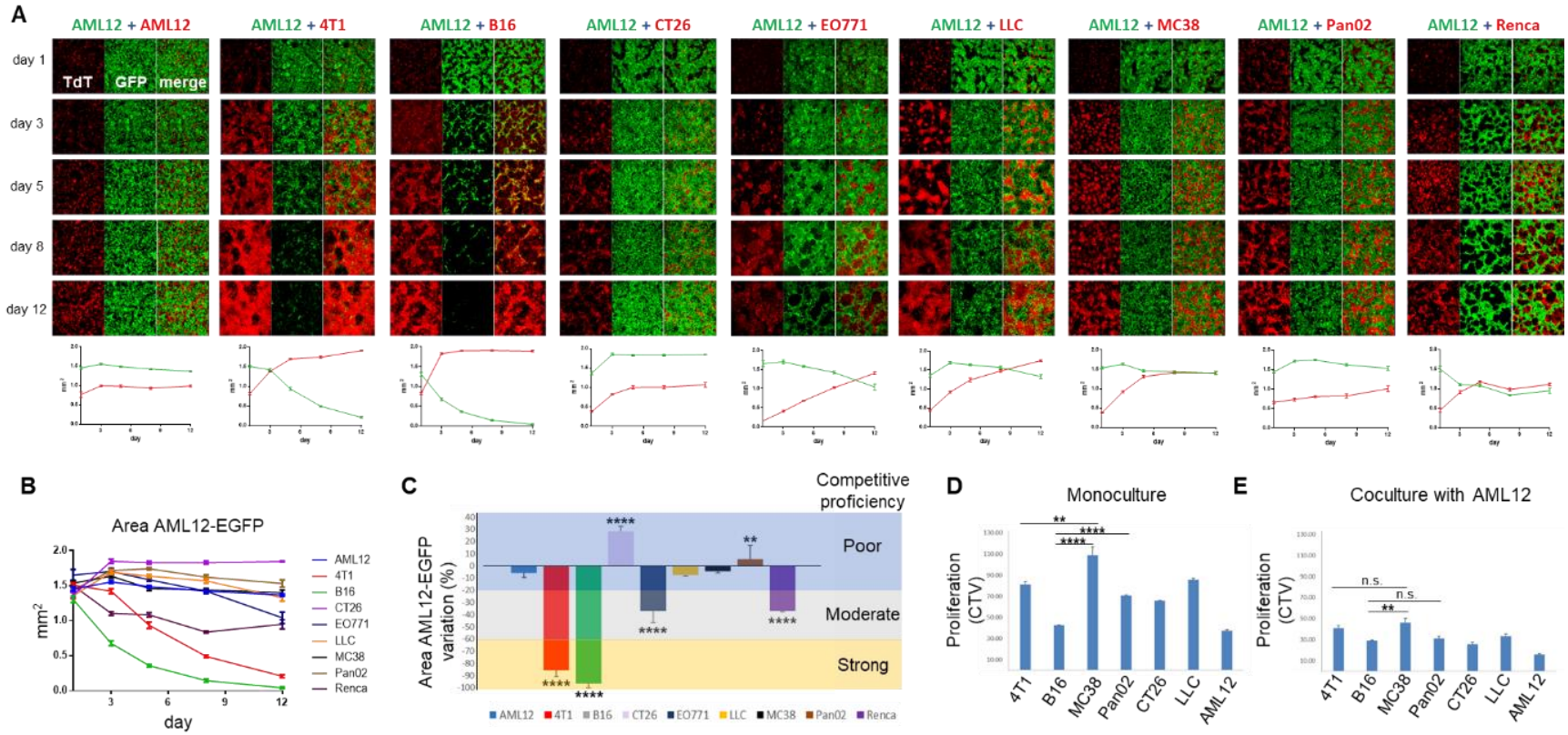
A
AML12 + AML12
AML12 + 4T1
AML12 + B16
AML12 + CT26
AML12 + EO771
AML12 + LLC
AML12 + MC38
AML12 + Pan02
AML12 + Renca
day 1
day 3
day 5
day 8
day 12
TdT
GFP
merge
B
Area AML12-EGFP
mm2
day
AML12
4T1
B16
CT26
EO771
LLC
MC38
Pan02
Renca
C
Competitive proficiency
Area AML12-EGFP variation (%)
Poor
Moderate
Strong
D
Monoculture
Proliferation (CTV)
E
Coculture with AML12
n.s.

Fig. 5: Competition between murine cancer cells and AML12 cells in 2D culture. **(A)** Representative images of AML12-EGFP cells in culture with eight murine cancer cell lines and control AML12 cells, expressing TdTomato (TdT). At the bottom, a graph plots the area per field of view of a 10x objective (y axis, mm^2) that is occupied over time (x axis, days) by AML12-EGFP cells (green curve) and the partner cell line (red curve). **(B)** The curves of AML12-EGFP cells from the whole experiment are plot together**.** On the right, a panel indicates the partner cell line and the color of the representative curve. **(C)** Variation of the area per field of view of EGFP, measured as the ratio between the area on day 12 and the area on day 1. Each color corresponds to a different partner of culture of AML12-EGFP cells, as indicated at the bottom of the graph. The variation obtained with each cancer cell line is compared with the one measured with AML12-TdT cells. Cancer cells are defined poor competitors when the loss of AML12-EGFP cells is ≤20%, and strong competitors when the loss is >60%. **(D)** Proliferation of tumor cells in monoculture. The y axis indicates the mean dilution of cell trace violet (CTV) 72 hours after seeding. The value of B16 cells is compared with that of MC38 cells and Pan02 cells, while the one of 4T1 cells is compared with that of MC38 cells. The experiment was done in triplicate, the graph shows the mean and the SEM. **(E)** Proliferation of murine cancer cells in culture with AML12-EGFP cells for 96 hours. Again, B16 cells are compared with MC38 cells and Pan02 cells, while 4T1 cells are compared with MC38 cells.

data not shown]. This behavior differs from what we observed with the strong competitor cells and with EO771 cells, which induced a continuous decrease in the total area of AML12 cells.

Similar to what we found with murine cancer cells, when we cultured six human cancer cell lines with AML12-EGFP cells, only Panc1 cells behaved as strong competitors, while HCT-116 cells resulted moderate competitors, and HeLa cells, J82 cells, MDA-MB-231 cells, and SK-MEL-28 cells were poor competitors [FIG. 6].

We next asked whether the different phenotypes that we observed were a consequence of the proliferation rate of cells. To assess this, we marked mouse tumor cells with Cell Trace Violet (CTV), and quantified by flow cytometry the dye dilution after 3 days of growth in monoculture, and 4 days in coculture with subconfluent AML12-EGFP cells. We found that the strong competitors, B16 cells and 4T1 cells, were not the most proliferative cell lines [FIG. 5D-E]. For example, B16 cells proliferated slower than MC38 cells, both in monoculture and to a lesser extent when in culture with AML12 cells, while they proliferated slower than Pan02 cells when in monoculture and at the same rate when in culture with AML12 cells. Similarly, 4T1 cells proliferated less than MC38 cells in monoculture, and had the same proliferation rate when in culture with AML12 cells.

3.3 Cancer cells compress and displace AML12 cells

To further characterize the dynamics of our cell competition assay, as well as to explain why the overall area occupied by AML12-EGFP cells and cancer cells is often higher than the area of the field of view, we analyzed the orthogonal organization of cells. Images were acquired with high magnification, and included both living cultures and samples stained with phalloidin and DAPI, to visualize the cell membrane and the nucleus, respectively. We found that, whereas AML12-EGFP

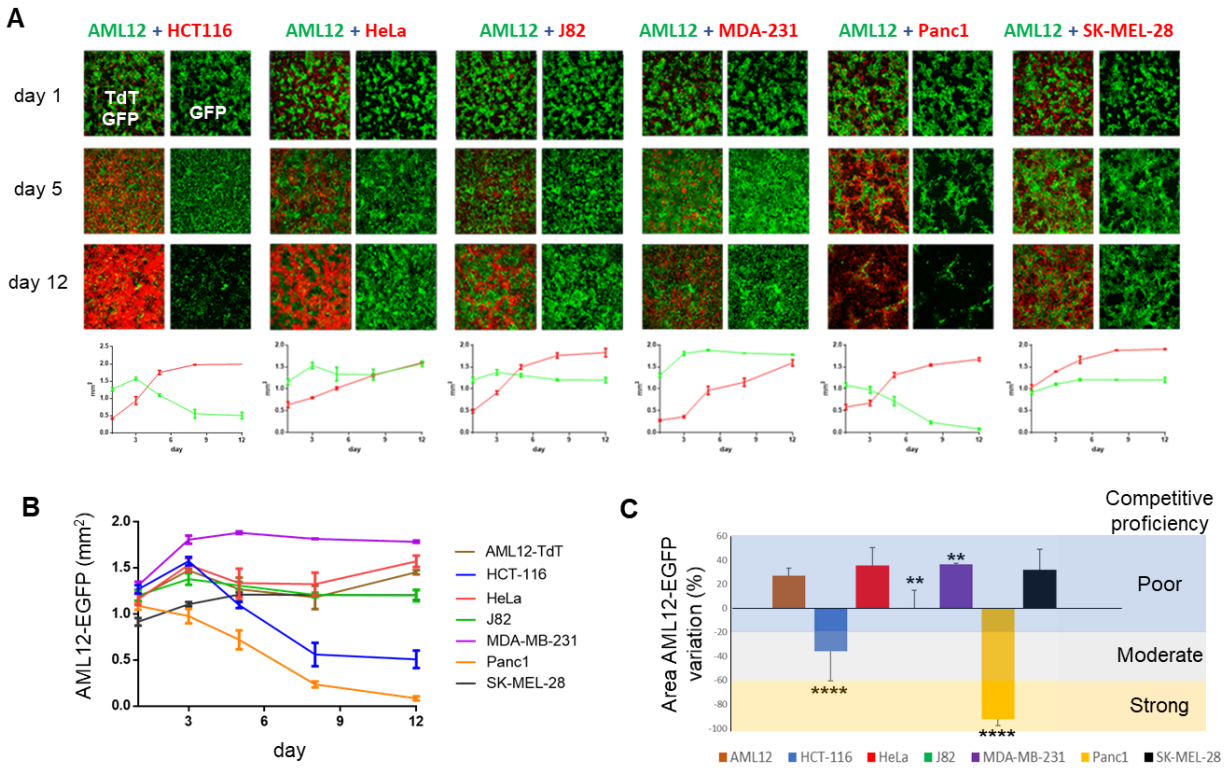

Fig. 6: Competition between human cancer cells and AML12 cells in 2D culture. **(A)** Representative images of AML12-EGFP cells in 2D culture with six human cancer cell lines expressing TdTomato (TdT). At the bottom, a graph plots the area per field of view that is occupied over time by AML12-EGFP cells (green curve) and the partner cell line (red curve). **(B)** The curves of AML12-EGFP cells from the whole experiment are plot together. **(C)** Variation of the area per field of view of EGFP and competitive proficiency of cancer cells, calculated as in FIG. 5C.

cells in culture with AML12-TdT cells were organized in a monolayer for the whole duration of the experiment, they frequently formed bi-layered and tri-layered structures at the interface with cancer cells [FIG. 7]. This phenomenon may indicate that cancer cells exert compressive forces on AML12 cells, especially when cell crowding is more advanced at day 9. To confirm this, we conducted particle image velocimetry to measure the deformation of AML12-EGFP cells over time in movies

acquired through time-lapse microscopy of 48 hours, from day 3 to day 5 of culture. Results show that both strong competitor and poor competitor cancer cells generate a great amount of compression on AML12 cells, with the highest intensity recorded in the culture with B16 cells [FIG. 8].

It has been reported that, in some forms of cell competition *in vitro*, loser cells are apically extruded from the monolayer, while winner cells colonize the surface of the dish [23,24]. In our experimental model, we found that the strong competitors, B16 cells and 4T1 cells, rapidly colonize the surface of the dish [FIG. 7]. In doing so, they displace AML12 cells, which can be found as multilayered clusters or laying on top of cancer cells. On the other hand, AML12-EGFP cells were broadly located on the surface of the dish when cultured with the other cancer cell lines, with tumor cells often growing on top of them. Importantly, although we could frequently observe AML12 cells laying on top of cancer cells, which may point towards their subsequent apical extrusion from the culture, this was massive only when AML12 cells were in culture with B16 cells.

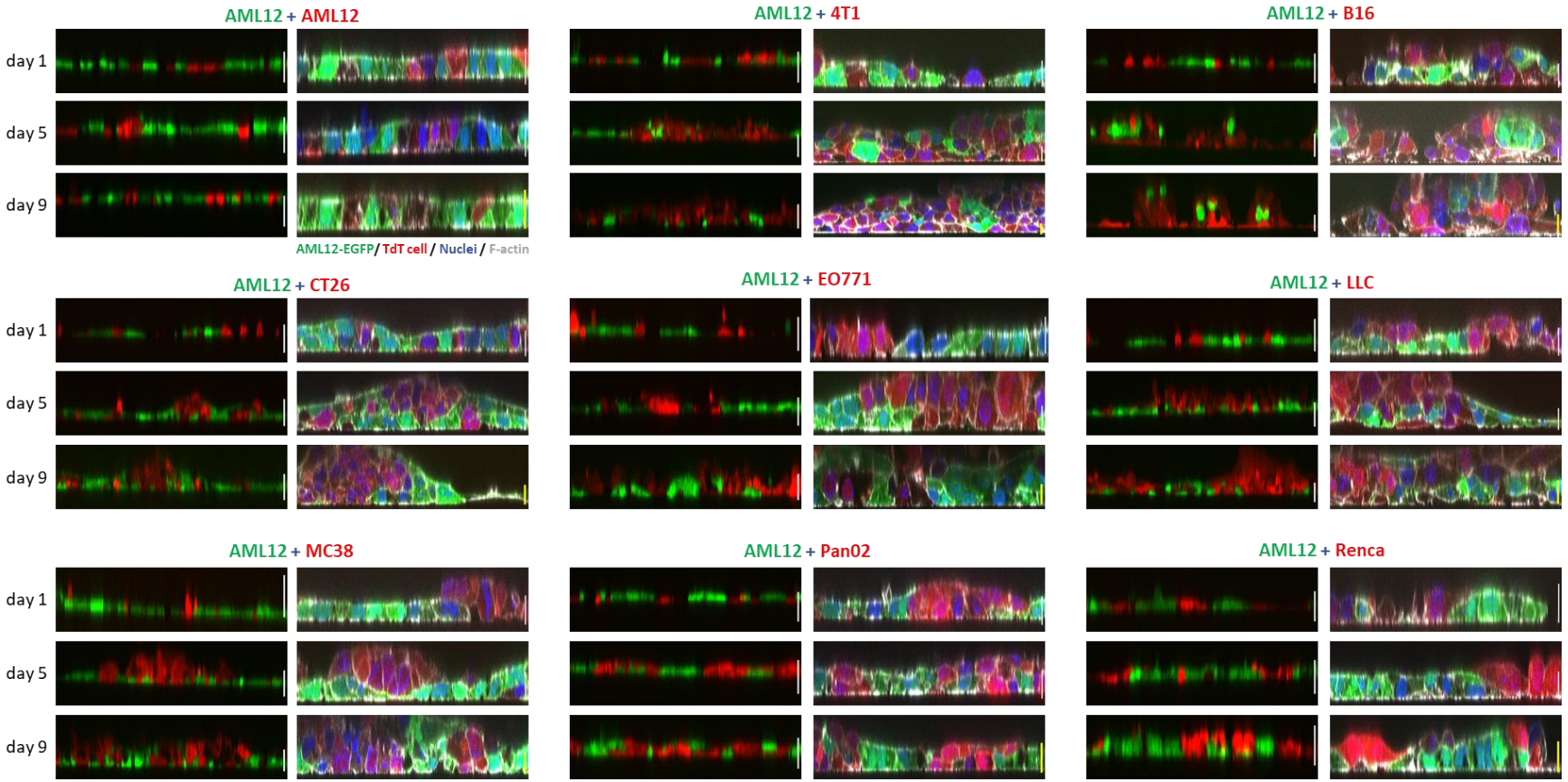
AML12 + AML12
AML12 + 4T1
AML12 + B16
day 1
day 5
day 9
AML12-EGFP/ TdT cell / Nuclei / F-actin
AML12 + CT26
AML12 + EO771
AML12 + LLC
AML12 + MC38
AML12 + Pan02
AML12 + Renca

Fig. 7: Orthogonal projection of cells competing in 2D. Representative images of the ZX plane of AML12-EGFP cells (green) in culture with murine cancer cells expressing TdTomato (TdT). For each coculture setting, the left panel shows images acquired from living cultures with a 20x objective (scale bar 20 µm), while the right panel shows images acquired with a 63x objective (scale bar 10 µm) after staining with phalloidin (grey), to stain the cell membrane, and DAPI (blue), to mark the nucleus.

3.4 Growing cells as spheroids alters the competitive behavior of some cancer cells compared to 2D culture

Culturing cells in 2D has a multitude of limitations concerning its inability to emulate *in vivo* conditions and provide physiological relevance [25]. Accordingly, we decided to further study the competitive phenotype of cancer cells in a 3D culture, by growing cell spheroids on top of an extracellular matrix. To track the variation of the population size of AML12-EGFP cells, we quantified the total volume per field of view that is occupied by EGFP. First of all, we observed that AML12 cells stop proliferating shortly after forming spheroids, while all the cancer cell lines proliferate incessantly. After 12 days of culture, we found that B16 cells and 4T1 cells maintained their state of strong competitors, resulting in an extensive (>75%) loss of AML12 cells of about 100% and 83%, respectively [FIG. 9]. Similarly, CT26 cells, MC38 cells, and Pan02 cells maintained their status of poor competitors, leading to a loss of AML12 cells ≤50%. We set this threshold based on the loss of AML12-EGFP cells that we observed with control AML12-TdT cells (about 27%).

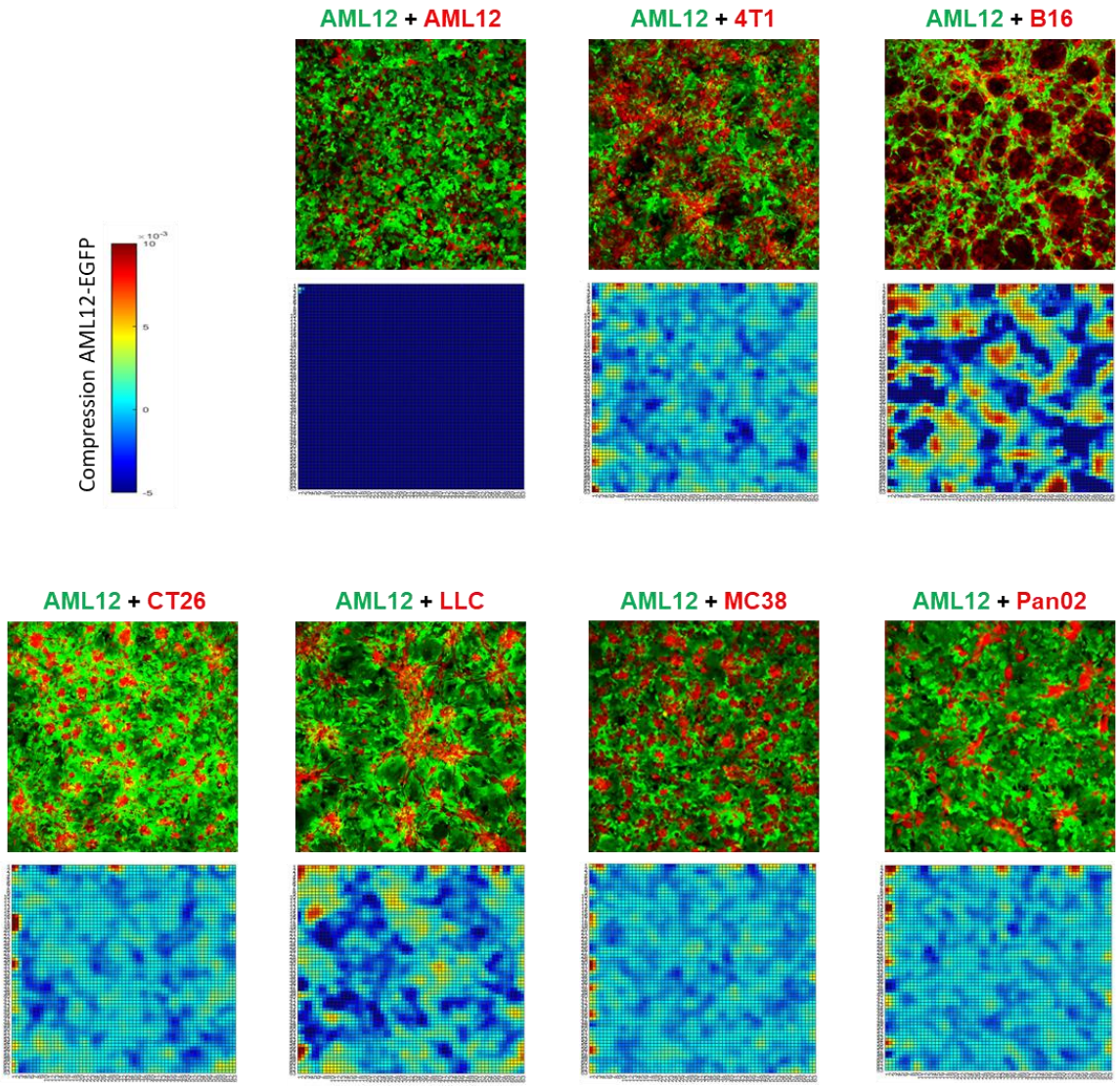

Fig. 8: Mechanical compression of AML12 cells in 2D culture. Particle image velocimetry analysis of movies obtained through live imaging from day 3 to day 5 of culture. The heat maps show the mean intensity of the compressive forces experienced by AML12-EGFP cells over time.

EO771 cells also confirmed their status as moderate competitors, generating a loss of AML12 cells of about 68%. Strikingly, although LLC cells were poor competitors when cultured in 2D, they became moderate competitors in 3D, inducing a loss of

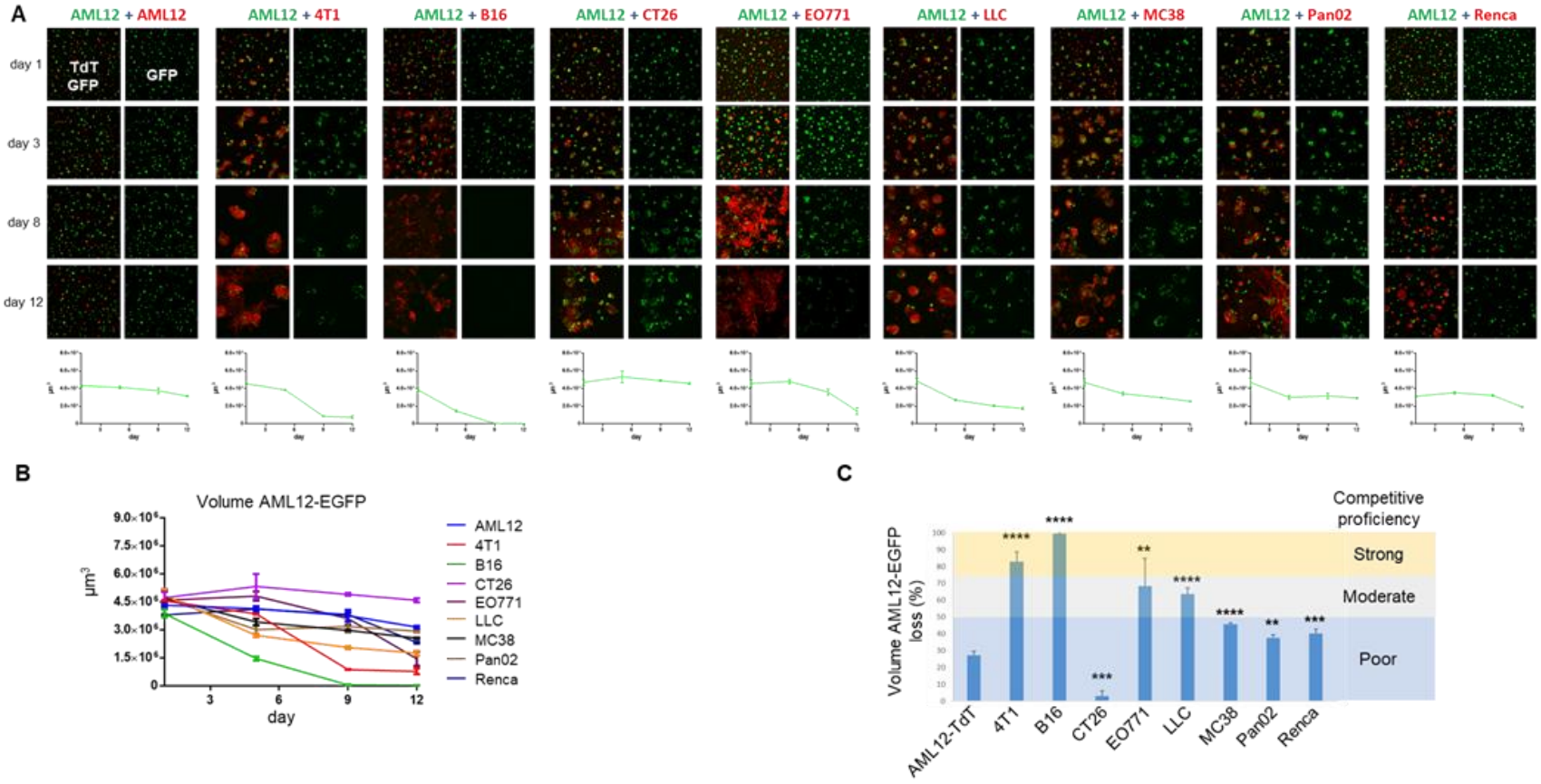
A
AML12 + AML12
AML12 + 4T1
AML12 + B16
AML12 + CT26
AML12 + EO771
AML12 + LLC
AML12 + MC38
AML12 + Pan02
AML12 + Renca
day 1
day 3
day 8
day 12
TdT GFP
GFP
B
Volume AML12-EGFP
µm³
day
AML12
4T1
B16
CT26
EO771
LLC
MC38
Pan02
Renca
C
Competitive proficiency
Strong
Moderate
Poor
Volume AML12-EGFP loss (%)
AML12-TdT
4T1
B16
CT26
EO771
LLC
MC38
Pan02
Renca

Fig. 9: Competition between mouse cancer cells and AML12 cells in 3D. (A) Representative images from the culture of AML12-EGFP cells with cancer cells and control AML12 cells, all marked with TdTomato (TdT), on top of Matrigel gel. At the bottom, a graph plots the total volume per field of view of a 10X objective (y axis, μm^3) that is occupied over time (x axis, days) by AML12-EGFP cells. **(B)** The curves of the volume per field of view of AML12-EGFP cells from the whole experiment are plot together**.** On the right a panel indicates the partner of culture of AML12-EGFP cells, and the color of the respective curve. (**C)** Quantification of the loss of AML-EGFP cells, measured as the ratio between the volume per field of view that is occupied by EGFP on day 12 and the value on day 1 (y axis). Each bar indicates a different partner of culture of AML12-EGFP cells, as listed at the bottom of the graph. The loss observed with each cancer cell line is compared to that obtained with AML12-TdT cells. Cancer cells are categorized as strong competitors when the loss of AML12-EGFP cells is more than 75%, while they are considered poor competitors when the loss is ≤50%.

AML12 cells of about 64%. Conversely, Renca cells were intermediate competitors in 2D, but became poor competitors in 3D.

Among human cancer cells, only HCT-116 behaved as strong competitors, while Panc1 cells were moderate competitors, and HeLa cells, J82 cells, MDA-MB-231 cells, and SK-MEL-28 cells maintained their status of poor competitors [FIG. 10].

Taken together, these data confirm that cancer cells display different degrees of supercompetition towards hepatocytes, which can vary depending on the culture system that is employed.

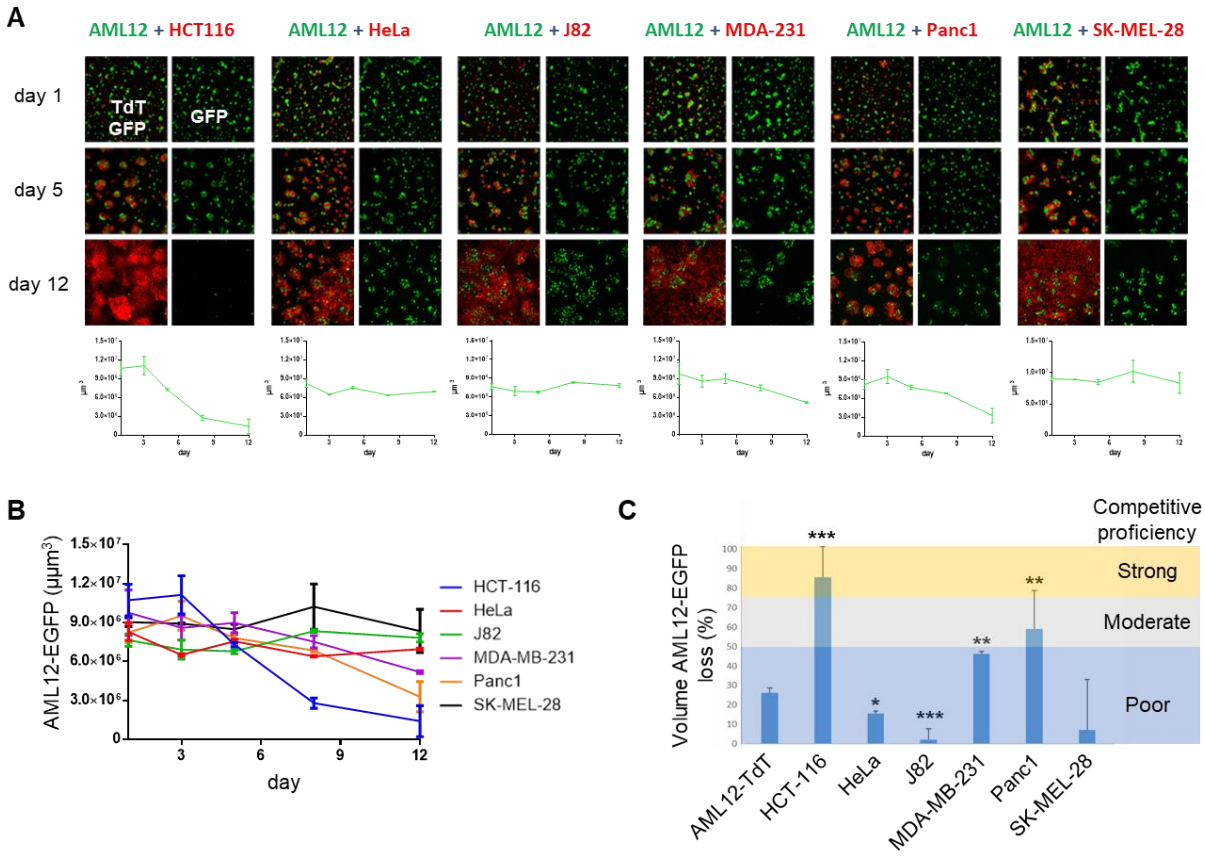

Fig. 10: Competition between human cancer cells and AML12 cells in 3D. (A) Representative images of AML12-EGFP cells growing as spheroids together with human cancer cells marked with TdTomato (TdT). At the bottom, a graph shows the total volume per field of view occupied over time by AML12-EGFP cells. **(B)** The curves of the volume per field of view of AML12-EGFP cells from the whole experiment are plot together. **(C)** Quantification of the loss of AML-EGFP cells and classification of the competitive proficiency of tumor cells as in FIG. 9C.

3.5 The competitive phenotype of cancer cells *in vitro* correlates with the behavior of liver metastasis

Experimental liver metastases were generated by injecting the murine cancer cell lines into the spleen of syngeneic adult mice. Animals were sacrificed 21 days after the injection of tumor cells, or earlier upon reaching humane endpoints. Results

show that the three cell lines with a consistent supercompetitive trait *in vitro*, which was coherent in 2D and 3D, were also the ones that generated more aggressive metastases. These required the sacrifice of animals on day 12 for B16 cells and EO771 cells, and on day 14 for 4T1 cells [Table 1 and FIG. 11A-C]. In contrast, none of the mice injected with LLC cells, MC38 cells, Pan02 cells or Renca cells appeared sick up to day 21, except for the presence of progressive hepatomegaly. Finally, mice injected with CT26 cells required sacrifice at day 14 due to massive hepatomegaly.

Morphologically, metastases deriving from 4T1 cells, B16 cells, and EO771 cells were endophytic and had an infiltrative growth pattern. Histologically, they were characterized by numerous cancer cells migrating inside the liver parenchyma, with marked intercalation with the hepatocytes and abundant single cell necrosis of the entrapped hepatocytes [Table 1, FIG. 11A and D]. In contrast, the poor competitors MC38 cells and Pan02 cells generated metastases with expansile and mixed growth patterns, respectively, with little to no migration of cancer cells within the liver, minimal to moderate intercalation with the hepatocytes, and minimal liver damage. The growth pattern of metastases deriving from LLC cells was also mixed, containing both expansile lesions and infiltrative tumor foci. Remarkably, although CT26 cells were poor competitors *in vitro*, they generated metastases that are morphologically similar to those from 4T1 cells and B16 cells. This again suggests

	4T1	B16	CT26	EO771	LLC	MC38	Pan02	Renca
Survival (days)	14	12	14	12	21	21	21	21
Tumor/liver ratio	Extreme	Very high	Very high	High	Medium	low	Medium	High
Growth pattern	Infiltrative	Infiltrative	Infiltrative	Infiltrative	Infiltrative/mixed	Expansile	Mixed	Infiltrative
Tumor-liver interface	Collective cancer cell migration	Collective cancer cell migration	Collective cancer cell migration	Ameboid cancer cell migration	Collective and ameboid cancer cell migration	Outward pushing	Outward pushing and collective migration	Outward pushing and collective cancer cell migration
Intercalation between cancer cells and hepatocytes	Marked	Marked	Marked	Marked	Marked	Minimal	Moderate	Mild
Liver damage	Marked single cell necrosis of entrapped hepatocytes	Marked single cell necrosis of entrapped hepatocytes	Marked hepatocellular vacuolation and hyperplasia, marked inflammation	Mild single cell necrosis of entrapped hepatocytes	Mild single cell necrosis of entrapped hepatocytes; moderate compressive/ischemic necrosis	Moderate compressive/ischemic necrosis	Mild hepatocellular hyperplasia	Minimal

Table 1: Histopathology of liver metastases. Morphological description of experimental liver metastases in syngeneic adult mice. Liver sections were stained with haematoxylin and eosin, and were studied by a veterinary pathologist.

that, in some cases, the competitive behavior of cancer cells is context-dependent, and differs depending on whether cells grow *in vitro* or *in vivo*.

When we stained the liver sections with an anti-cCasp3 antibody, we could only detect a minimal number of apoptotic hepatic cells at the tumor border [FIG. 11E]. Nonetheless, 4T1 cells, B16 cells and EO771 cells tended to generate an increased number of cCasp3-positive cells compared to the other cancer cell lines, although this was statistically significant only when compared to MC38 cells. Importantly, these results must be interpreted in the context of the marked intercalation that we observed between five of the cancer cell lines and hepatocytes [Table 1]. This may have limited the distinction of apoptotic hepatocytes that are mixed with cancer cells within the periphery of the tumor.

3.6 Molecular analysis

Having described the phenotype of the competition between cancer cells and hepatocytes, we next moved towards a deeper characterization of the molecular mechanisms that promote the process. First, we sought to determine the amount of AML12-EGFP cells undergoing apoptosis during culture with cancer cells in 2D.

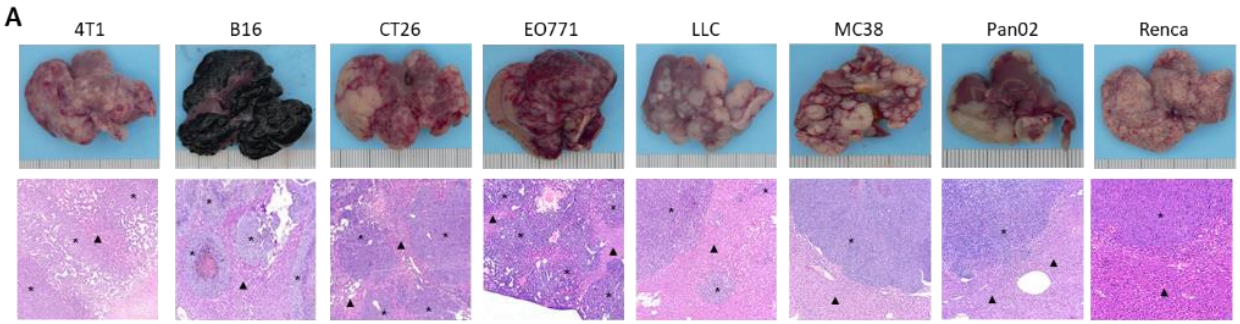
A
4T1
B16
CT26
EO771
LLC
MC38
Pan02
Renca

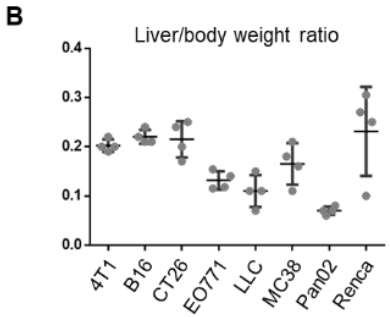
B
Liver/body weight ratio
0.4
0.3
0.2
0.1
0.0
4T1
B16
CT26
EO771
LLC
MC38
Pan02
Renca

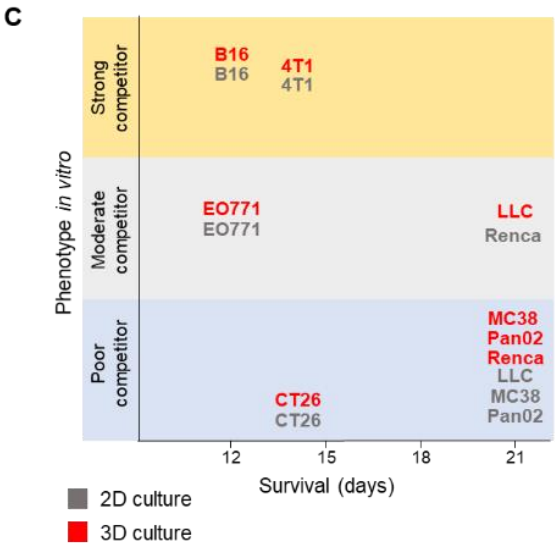
C
Phenotype in vitro
Strong competitor
Moderate competitor
Poor competitor
B16
B16
4T1
4T1
EO771
EO771
LLC
Renca
MC38
Pan02
Renca
LLC
MC38
Pan02
CT26
CT26
12
15
18
21
Survival (days)
2D culture
3D culture

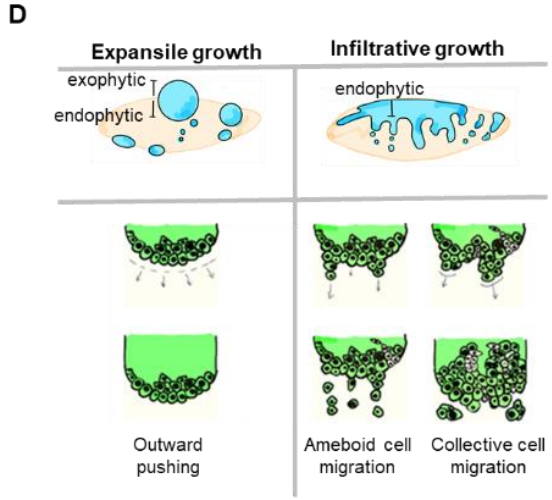
D
Expansile growth
Infiltrative growth
exophytic
endophytic
endophytic
Outward pushing
Ameboid cell migration
Collective cell migration

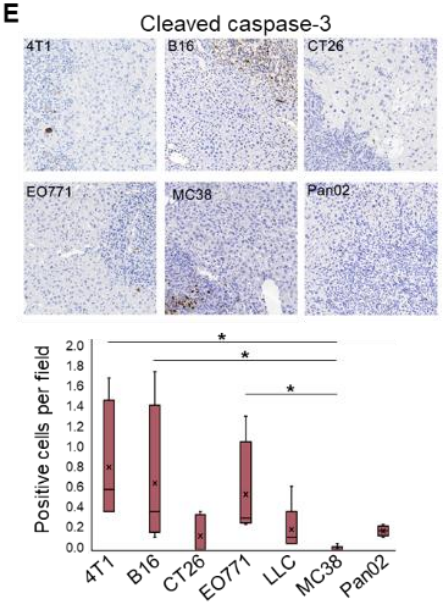
E
Cleaved caspase-3
4T1
B16
CT26
EO771
MC38
Pan02
Positive cells per field
2.0
1.8
1.6
1.4
1.2
1.0
0.8
0.6
0.4
0.2
0.0
4T1
B16
CT26
EO771
LLC
MC38
Pan02

Fig. 11: Experimental liver metastasis. **(A)** Top row: representative images of liver metastases. Lower row: representative images of liver sections stained with hematoxylin and eosin. Tumor foci are marked with an asterisk, while liver parenchyma with a triangle. **(B)** The tumor load is quantified by dividing the weight of the liver for the weight of the body on the day of sacrifice (y axis). **(C)** The graph plots together the survival of the animals with the competitive competence of cancer cells towards AML12 cells from FIG. 5C (gray) and FIG 9C (red). **(D)** Schematic illustration of tumor expansile growth (left) and infiltrative growth (right) in liver metastases, macroscopically (upper panel) and histologically, at the interface of cancer cells with liver (lower panel). **(E)** Top panel: representative images of liver sections stained with an anti-cleaved caspase-3 (cCasp-3) antibody and counterstained with hematoxylin. Lower panel: quantification of the number of cCasp-3 positive liver cells at the tumor border per field of view (y axis). The values obtained in metastases deriving form 4T1 cells, B16 cells and EO771 cells are compared with those of metastases deriving from CT26 cells, LLC cells, MC38 cells and Pan02 cells.

After three, six, and nine days of culture, we collected cells and stained them with Annexin V and propidium iodide (PI) for flow cytometry analysis. To our surprise, we could not detect increased apoptosis of AML12-EGFP cells with any cancer cell line compared to control AML12-TdT cells, with the exception of day 3 of culture with B16 cells, but not day 6 and day 9 [FIG. 12A]. This suggests that processes different from apoptosis mediate the elimination of AML12 cells in this context. For example, the apical extrusion from the culture might be particularly relevant when AML12 cells are in culture with B16 cells [FIG. 7]. Furthermore, the involvement of other forms of regulated cell death, towards which the assay that we used is not sensible, can not be excluded.

We next asked whether classical mediators of cell competition, such as myc [6] and Flower (Fwe) fitness fingerprints [10,11], contribute to determining the competitive outcome. We analyzed the basal mRNA expression levels of myc and the four Fwe isoforms in cells growing in 2D. We found that, except B16 cells, all cancer cell lines expressed significantly more myc compared to AML12 cells, with 4T1 cells and EO771 cells expressing the highest levels [FIG. 12B]. By contrast, the expression of Fwe^{Win} isoforms, Fwe2 and Fwe4 [11], was not higher in 4T1 cells, B16 cells or EO771 cells compared to AML12 cells.

We reasoned that the expression of myc and Fwe in cells that are actively competing might differ from that in basal conditions. Accordingly, we quantified the mRNA levels of myc and Fwe of AML12 cells in culture with B16 cells or Pan02 cells. Again, myc levels were higher in Pan02 cells and lower in B16 cells compared with partner AML12 cells, while Fwe^{Win} isoforms were not upregulated in either cancer cell line [FIG. 12C].

3.7 Mechanistic analysis

We asked whether cancer cells need to physically interact with AML12 cells to outcompete them, or whether secreted soluble factors are responsible for this effect. To test this, we cultured AML12 cells both in 2D and 3D, and treated them with the conditioned media derived from cancer cells. Results show no major effect on the

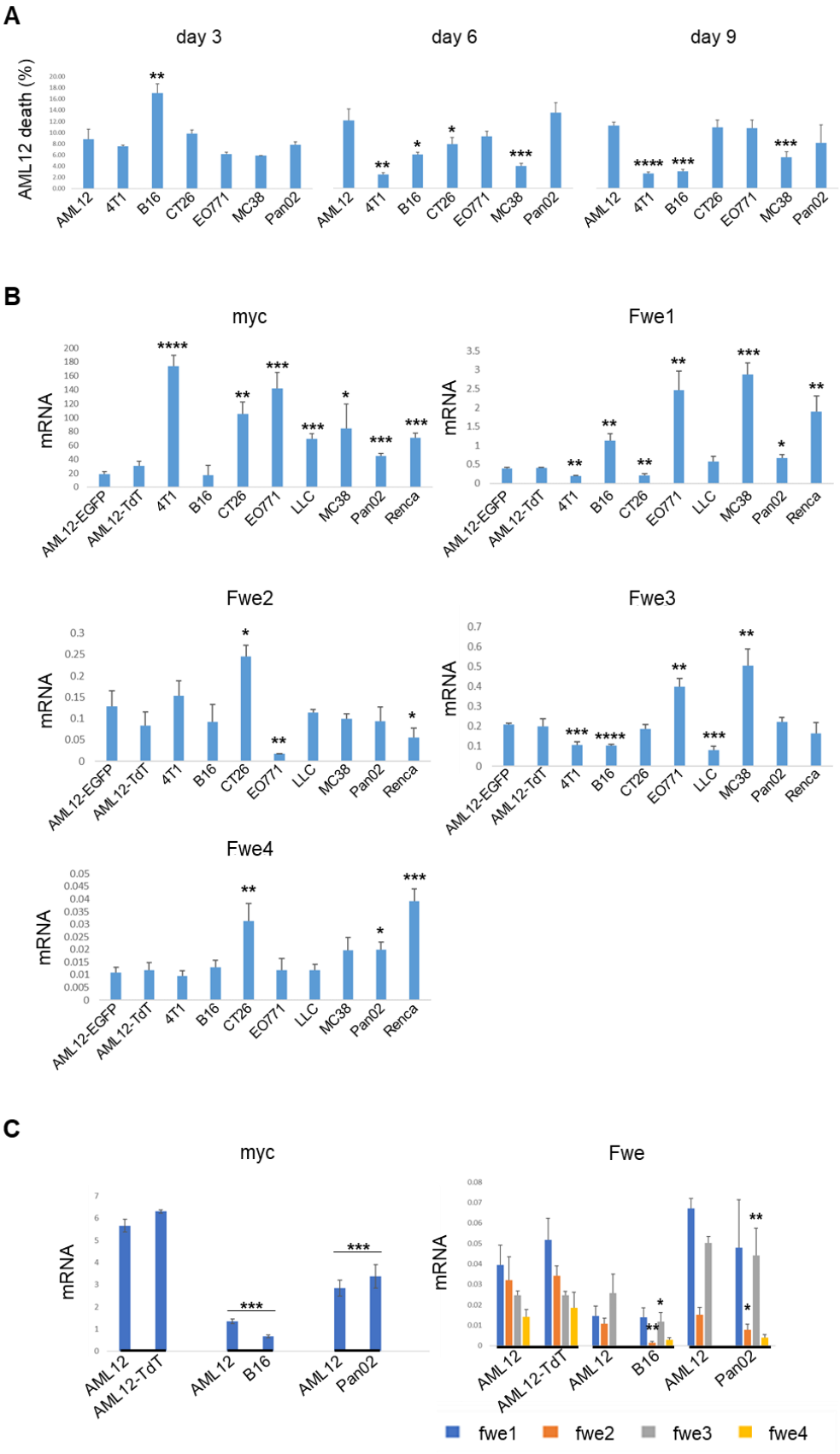
A
day 3
day 6
day 9
AML12 death (%)
AML12
4T1
B16
CT26
EO771
MC38
Pan02
B
myc
Fwe1
Fwe2
Fwe3
Fwe4
mRNA
AML12-EGFP
AML12-TdT
LLC
Renca
C
Fwe
fwe1
fwe2
fwe3
fwe4

Fig. 12: Molecular analysis of cells competing in 2D culture. **(A)** Quantification by flow cytometry of AML12-EGFP cells undergoing apoptosis after 3 days, 6 days and 9 days in culture with cancer cells. The value is obtained through the sum of the percentage of AML12-EGFP cells that are positive for Annexin V, propidium iodide (PI), or both. The percentage of apoptotic AML12-EGFP cells recorded for each cancer cell line is compared with that obtained with control AML-TdT cells. **(B)** mRNA expression of myc and Flower (Fwe) isoforms by real-time PCR (RT-PCR). The y axis indicates the expression levels of the gene after normalization for the expression 18S**. (C)** mRNA expression of myc and Fwe in cells cultured together for 3 days. The y axis indicates the expression levels after normalization for 18S expression, the x axis indicates the cell pair in culture with a bold line.

population size of AML12 cells, independently of the cancer cell line that generated the conditioned media [FIG. 13A]. To test whether factors that are produced by cancer cells specifically when in culture with AML12 cells are involved, we treated AML12 cells with the supernatant from cancer cells growing with AML12 cells. Again, we found no significant effect on AML12 cells, neither in 2D nor 3D [FIG. 13B]. These data imply that the competition between cancer cells and AML12 cells is contact-dependent.

We next assessed whether AML12 cells were competing with cancer cells for trophic factors that are present in the media. Fetal bovine serum (FBS) is the source of growth factors in the culture media, accordingly we cultured cells for 10 days in media containing either a low concentration of FBS (1%) or a high concentration (20%). We observed that B16 cells and 4T1 cells remain strong competitors while

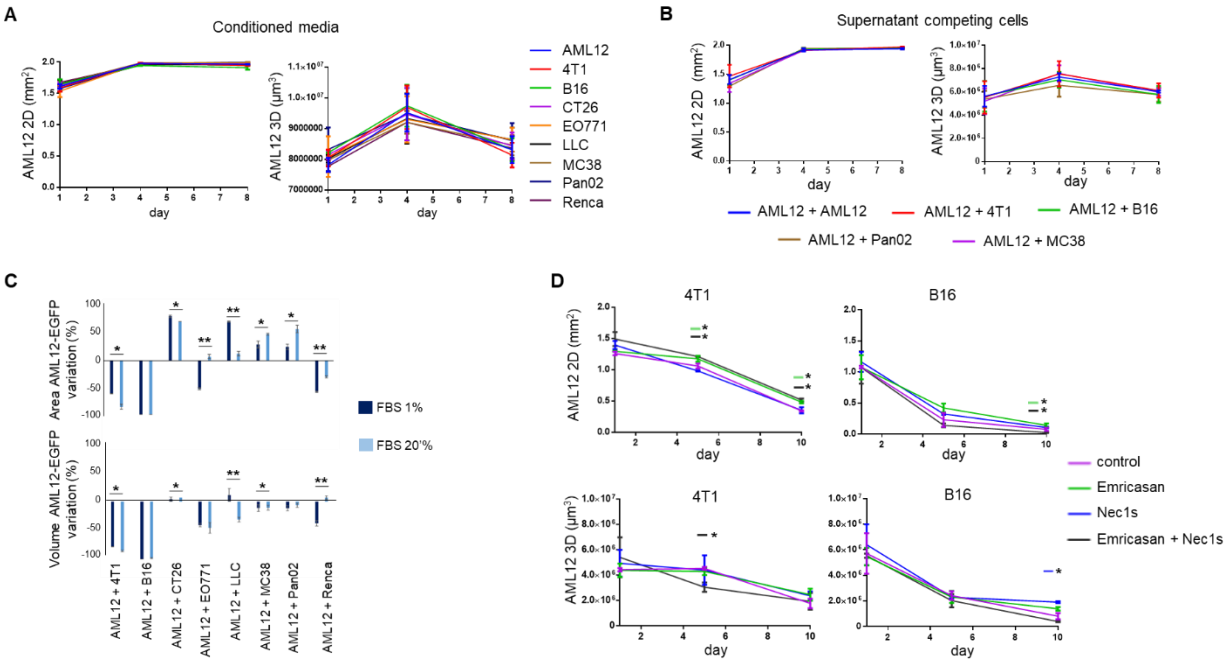

Fig. 13: Mechanistic study of tumor supercompetition. **(A)** The graphs show the total area (left, cells cultured in 2D) and the total volume (right, cells cultured in 3D) per field of view of AML12-EGFP cells during treatment with conditioned media from cancer cells, as listed on the right. **(B)** Total area (left, cells cultured in 2D) and total volume (right, cells cultured in 3D) per field of view that are occupied by AML12-EGFP cells during treatment with the supernatant from competing cells, ad indicated on the bottom. **(C)** Variation between day 10 and day 1 of the total area per field of view (upper panel, 2D culture) and the total volume per field of view (lower panel, 3D culture) of AML12-EGFP cells in culture with murine cancer cells with growth media containing either high fetal bovine serum (FBS) (dark blue) or low FBS (light blue). **(D)** Total area (upper panel, cells cultured in 2D) and total volume (lower panel, cells cultured in 3D) per field of view that are occupied by AML12-EGFP cells during 10 days of culture with B16 cells and 4T1 cells, in the presence of Emricasan (10 µM), Nec1s (20 µM), Emricasan + Nec1s, or vehicle. The area and the volume detected in each treatment arm at day 5 and at day 10 are compared with those of control.

CT26 cells, MC38 cells and Pan02 cells remain poor competitors, independently of the concentration of FBS in the media [FIG. 13C]. Notably, EO771 cells became poor competitors in 2D culture with high FBS, however this was not evident when they were cultured in 3D.

Caspase-dependent cell death has been reported to mediate the elimination of loser cells in numerous competitive scenarios [9,10,26]. Although our experiment with Emricasan in liver metastases was negative, we asked whether caspase-dependent cell death was promoting the elimination of AML12 cells. We cultured AML12 cells with the strong competitors, 4T1 cells and B16 cells, in the presence of Emricasan or vehicle. Results indicate that caspase inhibition alone confers only marginal protection to AML12 cells, which is evident specifically when cells were cultured in 2D but not in 3D [FIG. 13D]. Importantly, in some situations, when the activity of caspases is inhibited, a form of regulated necrosis called necroptosis is induced in response to the stimulation of death receptors [28]. Moreover, recent findings advocate that necroptosis is responsible for the elimination of loser cells in a model of cell competition driven by the expression of mutant p53 [29]. Accordingly, we tested whether the inhibition of necroptosis with Nec1s, a potent RIPK1 inhibitor, as well as the combination of Emricasan and Nec1s can prevent the elimination of AML12 cells. Again, either treatment produced minimal to no effect on the outcome of the competition [FIG. 13D], suggesting that neither caspase inhibition nor the

block of necroptosis are sufficient to rescue the elimination of AML12 cells in this context.

3.8 Cell cannibalism plays a minor role in the outcompetition of hepatocytes

The images from the experiment in FIG. 7 show that 4T1 cells occasionally contain fragments of AML12-EGFP cells within their cytosol, indicating the presence of cell cannibalism. This was not evident when AML12 cells were cultured with the other cancer cell lines. To directly quantify the presence of cell-in-cell phenomena in cells growing in 2D, we counted the number of single cells that were positive both for TdT and GFP at the flow cytometer. Overall, we found a low rate of double-positive cells, which was significantly higher than the one of control AML12-TdT cells only when AML12-EGFP cells were in culture with 4T1-TdT cells, EO771-TdT cells, and Pan02-TdT cells for 8 days, but not at day 3 [FIG. 14A].

To study the relevance of cell cannibalism, we cultured the strongest competitors 4T1 cells, B16 cells and EO771 cells with AML12 cells in the presence of the ROCK inhibitor Y27632, a drug that is widely used to inhibit entosis and cell cannibalism. Results show that ROCK inhibition does not affect the outcompetition of AML12 cells when cultured with either cancer cell line in 2D [FIG. 14B], while significant protection is evident only when AML12 cells are cultured with 4T1 cells in 3D [FIG. 14C].

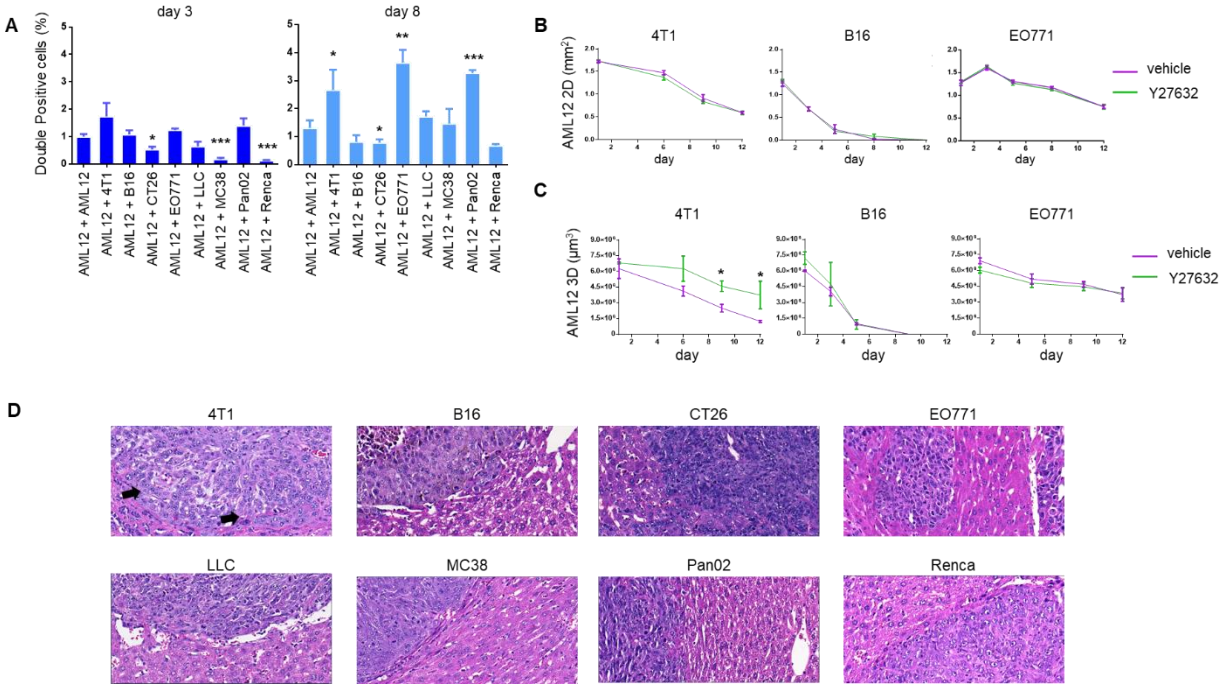

Fig. 14: Study of cell cannibalism. (A) Percentage of single cells that are positive for both EGFP and TdTomato (TdT) out of the AML12-EGFP population. The data derive from flow cytometry analysis after 3 days and 8 days of culture in 2D of AML12-EGFP cells with cancer cells expressing TdT. Each culture with cancer cells is compared to the one with AML12-TdT cells. **(B)** Total area per field of view that is occupied by AML12-EGFP cells during 12 days of culture in 2D with 4T1-TdT cells, B16-TdT cells and EO771-TdT cells, in the presence of Y27632 (10 µM) or vehicle. **(C)** Total volume per field of view of AML12-EGFP cells during 12 days of culture in 3D with 4T1-TdT cells, B16-TdT cells and EO771-TdT cells, with and without the addition of Y27632 to the growth media. **(D)** Representative images of liver sections from the experiment in FIG. 11. The black arrows indicate cancer cells showing features of cell cannibalism.

At last, the histological analysis of liver metastases revealed the general absence of cell-in-cell phenomena, with the exception of a minimal number of events in tumors deriving from 4T1 cells [FIG. 14D]. Taken together, these data suggest that cell cannibalism is a minor executioner of tumor supercompetition towards hepatocytes.

3.9 When the space is limited, the growth of poor competitor cancer cells is physically restrained by AML12 cells

To explain why, when growing in 2D, poor competitor cancer cells are unable to expand and colonize the culture, we increased the competitive level of MC38 cells and Pan02 cells by overexpressing membrane FasL [FIG. 15A]. We confirmed that the resulting overexpression of FasL was functional, as when AML12-EGFP cells were cultured with MC38L-TdT cells or Pan02L-TdT cells, they underwent significant apoptosis [FIG. 15B]. This was massive in the case of Pan02L cells, due to their higher expression of FasL compared to MC38L cells. As expected, the apoptosis of AML12 cells was completely prevented by the addition of Emricasan to the culture media.

Next, we seeded cells confluent in the presence of Emricasan or vehicle, and observed the competitive outcome. We found that, when the effect of FasL was not neutralized by the inhibition of caspases, AML12 cells were rapidly eliminated from the culture and cancer cells colonized all or a great part of the area [FIG. 15C and D]. On the contrary, in the presence of Emricasan, AML12 cells covered almost all the culture area, and cancer cells were unable to expand and colonize the culture. This suggests that AML12 cells physically constrain the growth of cancer cells when their competitive machinery is neutralized. Notably, this is not due to a direct

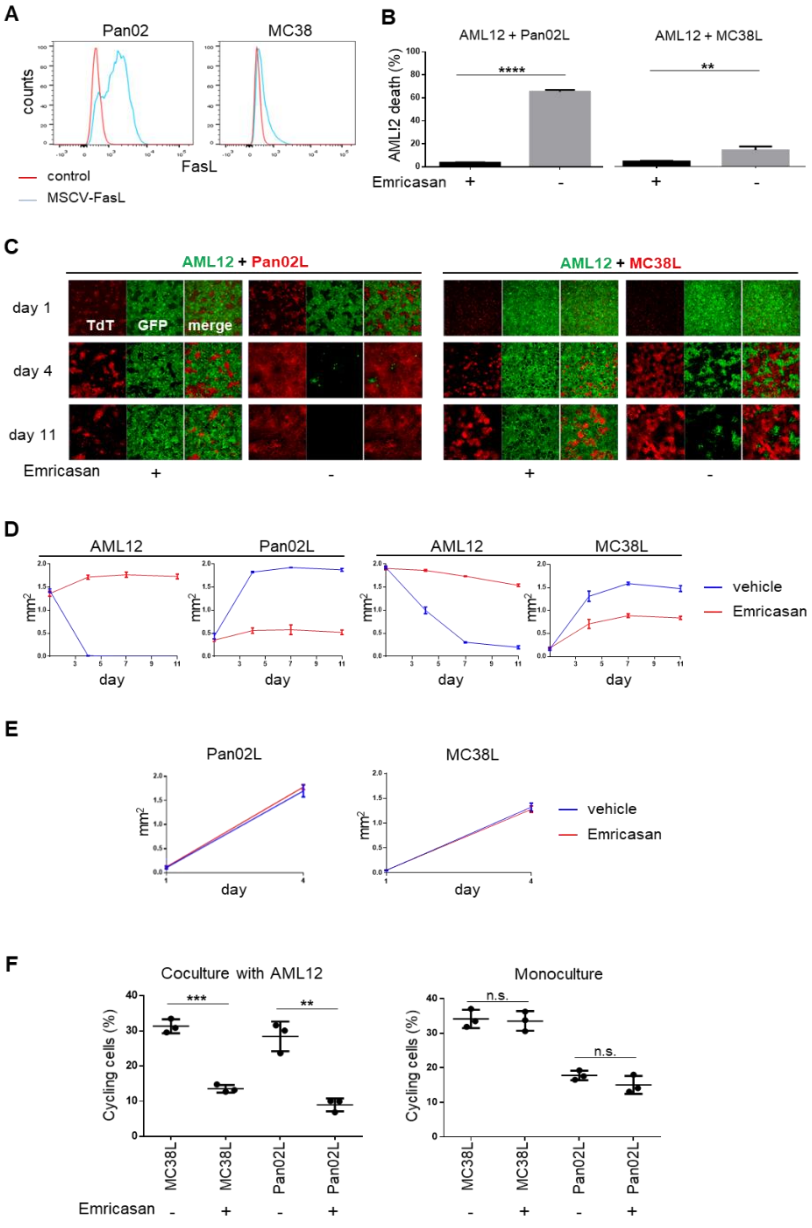

inhibitory effect of Emricasan on cancer cells, because their growth in monoculture was not affected by the treatment [FIG. 15E].

Fig. 15: Competition between AML12 cells and cancer cells overexpressing FasL. **(A)** Flow cytometry quantification of membrane FasL expression in MC38 cells and Pan02 after transduction with MSCV-FasL retrovirus. **(B)** Sum of the percentage of AML12-EGFP cells that are positive for Annexin V, propidium iodide (PI), or both, after 24 hours in culture with Pan02L-TdT cells and 48 hours in culture with MC38L-TdT cells. Emricasan (10 μM) or vehicle were added to the growth media at the moment of seeding. **(C)** Representative images of AML12-EGFP cells in culture with Pan02L-TdT cells and MC38L-TdT cells, with and without Emricasan. **(D)** Area per field of view occupied by AML12-EGFP cells and cancer cells from the experiment in **C**. **(E)** Area per field of view of MC38L-TdT cells and Pan02L-TdT cells in monoculture. **(F)** Cell cycle analysis of cancer cells in culture with AML12-EGFP cells (left panel) and in monoculture (right panel). The rate of cycling cells is calculated as the sum of the percentages of cells in phase S and cells in phase G2.

Next, we analyzed the cell cycle of MC38L cells and Pan0L cells in culture with subconfluent AML12-EGFP cells, in the presence of Emricasan or vehicle. Notably, preventing the elimination of AML12 cells lead to an important decrease in the number of cancer cells progressing from the phase G0/G1 to the phases S and G2 of the cell cycle [FIG. 15F]. The treatment with Emricasan had no major effect on the cell cycle dynamics when cancer cells were seeded scarce in monoculture. This suggests that, when cancer cells are unable to outcompete AML12 cells for space, they arrest their growth. Taken together, these results show that, when the vital space is constrained, the elimination of healthy cells is critical for the expansion of cancer.

DISCUSSION

Established cancer represents the late phase of a series of events that often begin many years earlier, and that lead the transformed cells to progressively acquire new traits and functions. Among these, the development of a supercompetitor state and the degree of such feature have been proposed to be crucial in defining the behavior and the morphology of the tumor [7,8,13,31]. In our research, we focused on the competitive interactions between cancer cells and hepatocytes for different reasons. First, the liver is a common metastatic site for numerous types of cancer, meaning that cell competition between cancer cells and hepatocytes is a relevant phenomenon. Second, the liver is mostly constituted by solid parenchyma, which makes it an ideal organ for the study of tumor infiltrative growth. Third, hepatocytes are the predominant cellular population in the liver, constituting up to 80% of the liver mass [32]. Hence, we thought that their competitive interaction with cancer cells might work as a surrogate for predicting what happens in liver metastases.

Although cancer cells are considered to be intrinsically supercompetitors, we found that a good proportion of cancer cell lines are indeed poor competitors towards hepatocytes *in vitro*. In fact, among murine cancer cell lines, only two out of eight were strong competitors and one was moderate competitor both in 2D culture and 3D culture. Three cell lines were poor competitors both in 2D culture and 3D culture, and two were poor competitors either in 2D or in 3D culture. Among human cancer

cell lines, four out of six were poor competitors both in 2D culture and 3D culture, while there was only one strong competitor cell line per growth condition. Importantly, our data show that the competitive strength of cancer cell lines can change between 2D culture and 3D culture. This might be due to the different competitive pressures that take place among cells growing as spheroids compared to cells growing on a plastic surface with a limited area of growth. This finding has relevant implications in the field, since an amount of data describing the competition of mammalian cells *in vitro* have been derived from cells cultured only in 2D [6,10, 24,33-35].

Our data show that cancer cells exert significant mechanical compression upon AML12 cells when cultured in 2D. This was highest in the culture with the strong competitor B16 cells, suggesting that mechanical cell competition might be particularly relevant in this tumor model. In line with previous findings in other experimental settings [23,24,33], we also found that loser cells (AML12) might be eliminated by apical extrusion, although we did not specifically assess this with time-lapse microscopy.

Our data show that the intrinsic competitive competence of cancer cells towards hepatocytes correlates with the behavior of liver metastases in terms of aggressiveness and morphology. Cancer cells that were consistently supercompetitors *in vitro* generated aggressive metastases with an infiltrative growth

pattern. On the contrary, all but one of the remaining five cancer cell lines resulted in a more indolent disease, which in three cases displayed expansile or mixed growth. To our knowledge, this represents the most concrete evidence that has been produced, to date, supporting the existence of a link between tumor supercompetition and infiltrative growth in mammals.

We questioned the involvement of different molecular mediators and mechanistic processes that have been described to play important roles during cell competition. However, we were not able to isolate a leading tool that was responsible for the elimination of hepatocytes. Nonetheless, our data show that the competition between cancer cells and AML12 cells is contact-dependent, does not rely on apoptosis for the elimination of AML12 cells, and is not driven by the supply of trophic factors. Although caspase-dependent cell death appears to be a common executioner of cell competition, we found that the inhibition of caspases did not prevent the elimination of hepatocytes, both *in vitro* and in liver metastases. This means that other molecular mechanisms take part in the execution of this task, which might vary depending on the tumor type. Among these, our data suggest that a minor role may be played by cell cannibalism.

Finally, in a model of supercompetition due to the overexpression of FasL, we show that when the competitive force of cancer cells is neutralized, they struggle to expand. As a consequence, they arrest the cell cycle progression into a quiescent state. This

indicates that the persistence of AML12 cells hinders the growth of cancer cells, which in response decrease their proliferative rate. Importantly, besides inducing homeostatic stress on healthy cells, mechanical constraints and compression may also be detrimental to the tumor, and halt tumor expansion [82,83]. Our data seem to go towards this direction, and add evidence to the notion that preventing the elimination of healthy cells may constrain the growth of cancer [5].

In conclusion, this thesis represents a conceptual advance in the study of tumor infiltrative growth and its link with the supercompetitive trait of cancer cells. Although such correlation has been repeatedly asserted, adequate experimental evidence to support it has been lacking in mammalian tumors. The work presented in this thesis may function as a platform for future studies in the field, which may eventually lead to the identification of the molecular mechanisms that promote the elimination of healthy cells due to cancer aggression, in the liver as well as in other organs.

CONCLUSIONES

Los resultados obtenidos en esta tesis permiten obtener las siguientes conclusiones:

1. Aunque las células tumorales malignas se consideran intrínsecamente como supercompetidoras, tan sólo una fracción de las líneas celulares tumorales analizadas se comporta -con claro fenotipo- como competidora de los hepatocitos in vitro. El resto de las líneas analizadas muestran escaso, o incluso ningún, comportamiento como competidoras.

2. La fuerza con que compiten las líneas competidoras puede variar de un modelo de cultivo en 2D a uno en 3D. Esto se puede deber a diferencias en la "presión competitiva" que tiene lugar entre células que crecen como esferoides comparadas con aquellas que, pegadas a una superficie de plástico, tienen un área limitada de crecimiento. Este resultado tiene implicaciones relevantes en el campo de la competición celular ya que, hasta la fecha, este fenómeno se ha estudiado, exclusivamente, en cultivos 2D in vitro de células de mamíferos.

3. Las líneas celulares de tumores malignos ejercen una compresión mecánica significativa contra las células AML12 cultivadas en 2D. Dependiendo de la intensidad de la compresión, las células AML12 se ven forzadas a perder el contacto con el sustrato del cultivo y forman agregados en capas, especialmente en las regiones en las que contactan con células tumorales.

4. La competición intrínseca de las células tumorales frente a los hepatocitos afecta al comportamiento de las metástasis en el hígado, tanto en la agresividad, como en la morfología. Las líneas de células tumorales que se comportaron fehacientemente como supercompetidoras in vitro generaron metástasis agresivas y con un patrón infiltrativo. Por otro lado, todas las líneas tumorales (excepto una), que se comportaron como competidoras pobres in vitro, mostraron un patrón mucho más suave de la enfermedad, y se ajustaron a un modelo expansivo en vez de infiltrativo.

5. La competición entre células tumorales y células AML12 es dependiente del contacto, pero no depende de la apoptosis que conduce a la eliminación de células AML12, y tampoco se ve afectada por la presencia de factores tróficos. De hecho, aunque la muerte dependiente de caspasas es normalmente el activador de apoptosis en la competición celular, la inhibición de caspasas no impidió la eliminación de hepatocitos tanto in vitro, como en las metástasis del hígado in vivo. En consecuencia, deben ser otros los mecanismos que intervienen en dicha tarea que, a su vez, puede variar dependiendo del tipo de tumor. De esos posibles mecanismos, el canibalismo celular parece representar un papel menor.

6. En referencia al modelo de supercompetición debido a la expresión de FasL, se muestra que, cuando se neutraliza la fuerza competitiva de las células tumorales, dichas células tienen dificultades para expandirse. Como consecuencia, el ciclo

celular se detiene y las células se quedan en estado de reposo. Esta observación resulta coherente con la noción de que impedir la eliminación de células sanas obstaculiza el crecimiento del cáncer.

7. Esta tesis representa un avance conceptual en el estudio del crecimiento tumoral infiltrativo y pone de manifiesto la relación entre este y el carácter superpercompetitivo de las células tumorales malignas. Aunque, en el caso de células tumorales de mamíferos, dicha correlación se ha observado repetidamente, la evidencia experimental que la soporte era, hasta la fecha, escasa. Por esta razón, este trabajo puede servir como trampolín para futuros estudios en éste área que permitirán la identificación de los mecanismos moleculares que promueven la eliminación de células sanas, tanto en el hígado como en otros órganos, derivada de la agresión que representa el cáncer.

MATERIALS AND METHODS

6.1 Cell lines. AML12 cells (#CRL-2254), 4T1 cells (#CRL-2539) and LLC cells (#CRL-1642) were purchased from ATCC, PT67 cells from Clontech (#634401). All the other cell lines were a gift by research groups at Champalimaud Foundation. AML12 cells were grown in DMEM F12 supplemented with fetal bovine serum (FBS) 10%, insulin-transferrin-selenium 1X (Corning) and Dexamethasone 4 ng/mL. This media was also used for the experiments of AML12 cells in coculture with cancer cells. Cancer cell lines B16, EO771, LLC, MC38, HCT-116, MDA-MB-231 and Panc1 were grown in DMEM supplemented with FBS 10%, while 4T1, CT26, Pan02 and Renca in RPMI 10% FBS, and HeLa, J82 and SK-MEL-28 in EMEM 10% FBS.

6.2 Drugs. Emricasan (#S7775) and Y-27632 (#S1049) were purchased from Selleckchem, Nec1s was purchased from Biovision (#2263). All drugs were diluted in DMSO, and were added to the growth media starting 1 day after cell seeding, unless otherwise specified.

6.3 Generation of MSCV-FasL retroviral vector. The construct was generated as previously described (16). Briefly, total RNA was extracted from the thymus of a 4-weeks old C57BL/6 mouse using RNeasy Mini Kit (Qiagen), and complementary

DNA (cDNA) was generated from 1.6 µg of RNA using *SuperScript III First-Strand Synthesis System* (Invitrogen *#18080051*). Full length FasL DNA was amplified by using polymerase chain reaction (PCR) with the following primers: forward 5-CGGAATTCATGCAGCAGCCCATGAATTACCCATGT-3; and reverse 5-CGGAATTCTTAAAGCTTATACAAGCCGAAAAAGGT-3. The PCR product was cloned into MSCVpuro (Clontech *#634401*) vector at the EcoRI restriction site and confirmed by sequence analysis.

6.4 Generation of cells expressing EGFP or TdTomato. 293T cells were transfected using lipofectamine 3000 (Invitrogen *#L3000015*) with ViraPower packaging vectors (Invitrogen) and FUGW virus (Addgene, #14883) or FUtdTW virus (Addgene, #22478) backbones. The supernatant was collected after 48 hours, filtered through 0.45 µm, and directly used to transduce AML12 cells and cancer cells. Clones expressing EGFP (FUGW virus) and TdTomato (TdT, FUtdTW virus) were purified by fluorescence-activated cell sorting (FACS) at the flow cytometer.

6.5 Generation of cells overexpressing FasL. PT67 cells were transfected using lipofectamine 3000 with 6 µg of MSCV-FasL vector, and the supernatant was collected after 48 hours, filtered through 0.45 µm, and directly used to transduce MC38 cells and Pan02 cells. After 48 hours, puromycin (Sigma, #P8833) 3 µg/mL

was added to the growth media and replaced every 2 days for 8 days, then cells were collected and stained with an anti-FasL-PE antibody (Biolegend, #106605) 0.2 mg/mL in PBS 2% FBS for 30 minutes on ice, and purified by FACS. The resulting cells overexpressing FasL (MC38L and Pan02L) were transduced with the FUtdTW virus and purified by FACS.

6.6 Cell competition assay in 2D. AML12-EGFP cells ($1.8x10^5$ cells per well) were seeded with murine cancer cells expressing TdT and AML12-TdT cells ($6x10^4$ cells per well) in a 24-well μ-plate (Ibidi #82406). The growth media was replaced every day. In the experiments involving human cancer cell lines, these were seeded at $9x10^4$ cells per well. In the coculture with MC38L-TdT cells and Pan02L-TdT cells, AML12-EGFP were seeded $2x10^5$ cells per well, while cancer cells $1x10^4$.

6.7 Cell competition assay in 3D. AML12-EGFP cells ($4x10^4$ cells per well) were seeded with cancer cells expressing TdT and AML12-TdT cells ($2x10^4$ cells per well) on top of growth-factor-reduced Matrigel (Corning *#356252*; 160 μL per well) in a 24-well μ-plate, and covered with growth media containing 5% Matrigel. The media was replaced every day.

6.8 Proliferation analysis. Cells were stained with Cell Trace Violet (CTV; Invitrogen, #C34557), following manufacturer protocol for cells in suspension, and seeded in 2D in a 24-well plate, either alone ($4x10^4$ cells per well) or in coculture with confluent AML12-EGFP cells (cancer cells $6x10^4$ per well, AML12-EGFP cells $2.2x10^5$ per well). A part of cells was analyzed at the flow cytometer 30 minutes after staining to register the peak of CTV. The mean intensity of the CTV was quantified using FlowJo v10.8.1.

6.9 Conditioned medium experiment. The conditioned medium was generated by growing confluent cells in poor DMEM F12 for 24 hours. Supernatant was filtered through 0.45 μm and mixed with the complete growth media of AML12 cells to generate a 30% solution, which was then added to AML12-EGFP cells growing in 2D and in 3D starting from the day after seeding.

6.10 Supernatant from competing cells. AML12-EGFP cells were seeded in culture with cancer cells and AML12-TdT cells, and the supernatant of 24 hours was collected and filtered through 0.45 μm on day 3 of culture. It was then added to the media (30% solution) of AML12-EGFP cells cultured in 2D and in 3D starting from the day after seeding.

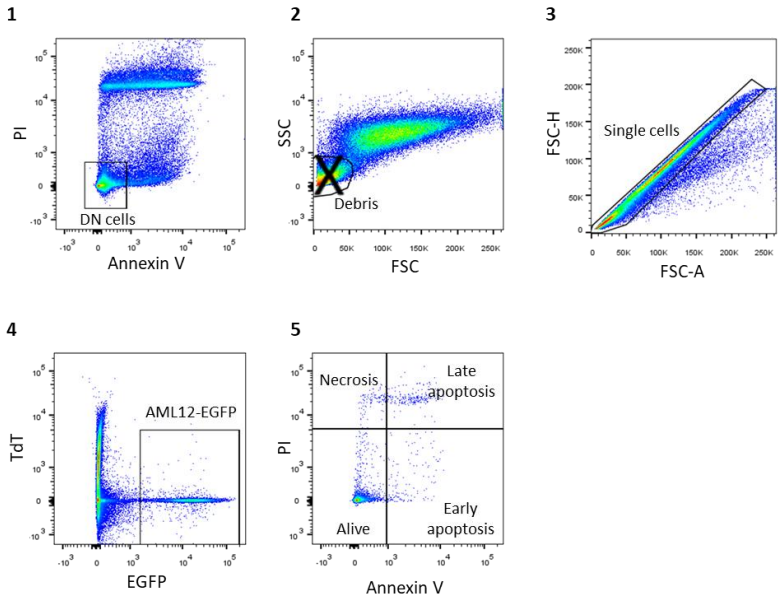

Fig. 16. Annexin V + PI data analysis. To identify cell debris, we displayed the Annexin V channel and the propidium iodide (PI) channel, and selected the double negative (DN) population (**1**). This was plotted according to the forward scatter (FSC) and the side scatter (SSC), and the events in the region with low FSC, which include cell debris, were excluded (ungated) (**2**). The resulting population was selected for single cells (**3**), then AML12-EGFP cells were gated (**4**) and analyzed for positivity to Annexin V and PI (**5**).

6.11 Phalloidin staining. Cells were fixed with PFA 4% in PBS for 15 minutes at room temperature, permeabilized with Triton X-100 0.1% in PBS for 15 minutes, and stained for 45 minutes with a solution of PBS 1% bovine serum albumin (BSA) containing Phalloidin Alexa Fluor Plus 647 (Invitrogen *#A30107*) 1X and DAPI (Thermofisher *#62248*) 1 µg/mL.

6.12 Annexin V assay. Cells were collected, washed, and stained for 15 minutes with Annexin V Pacific Blue (Biolegend *#640918*) 2 µL/100 µL and propidium

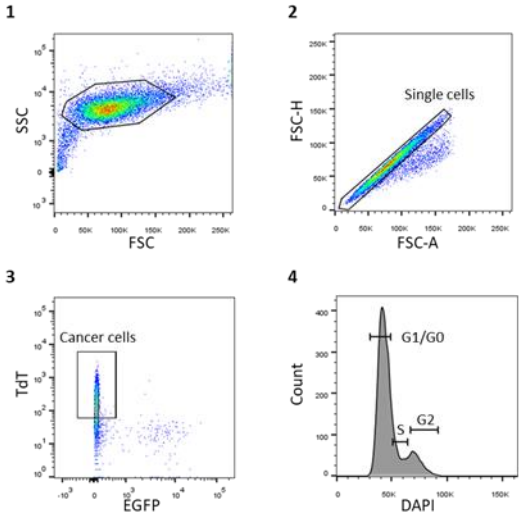

Fig. 17. Cell cycle analysis. Gating strategy for the study of the cell cycle in cancer cells expressing TdTomato (TdT).

iodide (Sigma *#P4170*) 20 µg/mL in Annexin V Binding Buffer (Biolegend *#422201*). Cells were then run in a flow cytometer and the results were analyzed using FlowJo as shown in FIG. 16. Experiments were conducted in triplicate and repeated three times.

6.13 Cell cycle analysis. MC38L-TdT cells and Pan0L-TdT cells ($1x10^4$) were seeded in coculture with AML12-EGFP cells ($1.8x10^5$) or in monoculture ($4x10^4$) in a 24-well plate. After 4 days, cells were collected, washed with PBS, fixed in PBS 2% PFA solution for 1 hour on ice, and permeabilized with ethanol 70% overnight at 4 degrees. Cells were rehydrated in PBS on ice for 10 min, then stained in 250 µL of cold PBS containing DAPI 10 µg/mL for 20 minutes and analyzed at the flow

cytometer. FlowJo was used to calculate the percentage of cells distributed in the phases G0/G1, S and G2 of the cell cycle [FIG. 17]. The experiment was done in triplicate and repeated twice.

6.14 RT-PCR. Total RNA was extracted using RNeasy Mini Kit (Qiagen #*74104*), and 1 µg of RNA was used to generate cDNA with QuantiTect Reverse Transcription kit (Qiagen #*205313*). For the RT-PCR reaction, PowerUp SYBR Green Master Mix (Applied Biosystems #*A25777*) was used, according to manufacturer protocol, with the following primers:

myc	Fw	TTTTTGTCTATTTGGGGACAGTG
	Rv	CATCGTCGTGGCTGTCTG
FasL	Fw	AAGAAGGACCACAACACAAATCTG
	Rv	CCCTGTTAAATGGGCCACACT
Fwe1	Fw	ATCTGTCGGCCAAGCTAACC
	Rv	GGGAAGTAACTGAGTCGCGT
Fwe2	Fw	GGAACTGTGAGGCCTGGAG
	Rv	GCCAGTGAAACAGCTCTCCT
Fwe3	Fw	CTGTCTTCTACTGCGGGCAT
	Rv	TTTCTGTTCGGCAGTCTCACA

Fwe4	Fw	TGCTAAATCCTGGGTGTCCC
	Rv	GAGGGTGGATAGTGACGCAG
GAPDH	Fw	GGATGCAGGGATGATGTTC
	Rv	TGCACCACCAACTGCTTAG
18S	Fw	GTAACCCGTTGAACCCCATT
	Rv	CCATCCAATCGGTAGTAGCG

6.15 Immunohistochemistry. Paraffin blocks were sectioned with a microtome to generate 5 µm thick sections, which were treated with xylene to remove paraffin, followed by rehydration with different gradients of ethanol and water. Heat-induced antigen retrieval was done with a steamer in sodium citrate pH 6 buffer for 20 minutes. Slides were then incubated for 1 hour at room temperature with anti-cleaved caspase-3 antibody (Cell Signaling Technology, #9661) diluted 1 to 300 in TBST 5% BSA, followed by a 15 min treatment with H_2O_2 3% to block endogenous peroxidase, and 1-hour incubation with HRP-bound goat anti-rabbit secondary antibody (Invitrogen, #31460). Finally, slides were stained with DAB substrate kit (VectorLabs, #SK-4100) and counterstained with hematoxylin.

6.16 Acute liver toxicity. Osmotic pumps (Alzet, model 1002) were filled with Emricasan, diluted in DMSO/PEG400 buffer, or only buffer, and implanted

subcutaneously on the dorsal region in adult C57BL/6 mice. After 2 days, 7 days and 12 days two mice from the Emricasan group and two control mice received intra tail vein injection of Jo2 antibody (BD Biosciences, #554255) 10 µg in 100 µL of PBS, and were sacrificed after 3 hours. The liver was extracted and fixed in PFA 4% for 48 hours, then embedded in paraffin.

6.17 Experimental liver metastases. Cancer cells were diluted in PBS, and $1x10^6$ cells in 100 µL were injected into the spleen of 10-weeks old syngeneic mice (C57BL/6 mouse for B16 cells, EO771 cells, LLC cells, MC38 cells and Pan02 cells; BALB/c mouse for 4T1 cells, CT26 cells, Renca cells), followed by splenectomy. After 21 days, or earlier upon reaching humane endpoints, animals were sacrificed, the liver was extracted and fixed in PFA 4% for 48 hours, then embedded in paraffin. In the experiments involving the use of osmotic pumps, these were implanted subcutaneously 3 days after the injection of cancer cells, and substituted after 14 days with new pumps. Mice were sacrificed 30 days after tumor challenge, or earlier upon reaching humane endpoints.

6.18 Microscopy imaging and analysis. For the experiments with cells *in vitro*, images were acquired with a Zeiss LSM 880 confocal microscope, using a 10x objective unless otherwise specified. The quantification of the area of fluorescent

cells was done with Fiji, and is based on the maximum intensity projection of each photo. The quantification of the volume of AML12-EGFP cells was done with Imaris v9.3.1. In all these experiments, cells were cultured in duplicate or more, and at least 4 photos per condition were acquired and used for the analysis.

Particle image velocimetry (PIV) was calculated using a previously developed PIVlab MATLAB routine [46]. To obtain higher accuracy in the displacement, two passes analysis was applied. For the first pass the interrogation window was set to 128 pixels with 50%, and for the second the window size was set to 64 pixels with 50% overlap. Parameters for this PIV were analysis boxes of 64 pixels (~44x44 mm), 50% overlap boxes. PIV displacements at time t were determined based on images t-25 and t+25min. Displacement maps were spatially filtered to remove noise coming from outliers. The convergence was calculated as the opposite of the field divergence and the average value over all frame is shown in the results.

For the study of liver sections, images were acquired with a ZEISS Axio Scan Z1 slide scanner, using a 10x objective.

6.19 Statistical analysis. For all the experiments, normal distribution was assumed, and two-tailed unpaired Student t-test was used for comparison of two groups, while ANOVA test was chosen for comparison of multiple groups.

BIBLIOGRAPHY

1. Zhao Y, Xu E, Yang X, Zhang Y, Chen H, Wang Y, Jin M. Tumor infiltrative growth pattern correlates with the immune microenvironment and is an independent factor for lymph node metastasis and prognosis in stage T1 esophageal squamous cell carcinoma. Virchows Arch. 2020;477(3):401-8.

2. Sashi R, Tomura N, Hashimoto M, Kobayashi M, Watarai J. Growth patterns of benign and malignant thyroid tumors estimated by CT. Radiat Med. 1997;15(1):7-11.

3. Moro CF, Bozóky B, Gerling M. Growth patterns of colorectal cancer liver metastases and their impact on prognosis: a systematic review. BMJ Open Gastroenterol. 2018;5(1):e000217.

4. Nakamura T, Matsumine A, Matsubara T, Asanuma K, Yada Y, Hagi T, Sudo A. Infiltrative tumor growth patterns on magnetic resonance imaging associated with systemic inflammation and oncological outcome in patients with high-grade softtissue sarcoma. PLoS One. 2017;12(7):e0181787.

5. Moreno E. Is cell competition relevant to cancer? Nat Rev Cancer. 2008;8(2):141-7.

6. Di Giacomo S, Sollazzo M, de Biase D, Ragazzi M, Bellosta P, Pession A, Grifoni D. Human Cancer Cells Signal Their Competitive Fitness Through MYC Activity. Sci Rep. 2017;7(1):12568.

7. Suijkerbuijk SJ, Kolahgar G, Kucinski I, Piddini E. Cell Competition Drives the Growth of Intestinal Adenomas in Drosophila. Curr Biol. 2016;26(4):428-38.

8. Eichenlaub T, Cohen SM, Herranz H. Cell Competition Drives the Formation of Metastatic Tumors in a Drosophila Model of Epithelial Tumor Formation. Curr Biol. 2016;26(4):419-27.

9. Levayer R, Dupont C, Moreno E. Tissue Crowding Induces Caspase-Dependent Competition for Space. Curr Biol. 2016;26(5):670-7.

10. Madan E, Pelham CJ, Nagane M, Parker TM, Canas-Marques R, Fazio K, Shaik K, Yuan Y, Henriques V, Galzerano A, Yamashita T, Pinto MAF,

Palma AM, Camacho D, Vieira A, Soldini D, Nakshatri H, Post SR, Rhiner C, Yamashita H, Accardi D, Hansen LA, Carvalho C, Beltran AL, Kuppusamy P, Gogna R, Moreno E. Flower isoforms promote competitive growth in cancer. Nature. 2019;572(7768):260-4.

11. Petrova E, López-Gay JM, Rhiner C, Moreno E. Flower-deficient mice have reduced susceptibility to skin papilloma formation. Dis Model Mech. 2012;5(4):553-61.

12. Levayer R, Hauert B, Moreno E. Cell mixing induced by myc is required for competitive tissue invasion and destruction. Nature. 2015;524(7566):476-80.

13. Vishwakarma M, Piddini E. Outcompeting cancer. Nat Rev Cancer. 2020;20(3):187-98.

14. Merino MM, Levayer R, Moreno E. Survival of the Fittest: Essential Roles of Cell Competition in Development, Aging, and Cancer. Trends Cell Biol. 2016;26(10):776-88.

15. Clavería C, Torres M. Cell Competition: Mechanisms and Physiological Roles. Annu Rev Cell Dev Biol. 2016;32:411-39.

16. Li H, Fan X, Stoicov C, Liu JH, Zubair S, Tsai E, Ste Marie R, Wang TC, Lyle S, Kurt-Jones E, Houghton J. Human and mouse colon cancer utilizes CD95 signaling for local growth and metastatic spread to liver. Gastroenterology 2009;137(3):934–44.

17. Yoong KF, Afford SC, Randhawa S, Hubscher SG, Adams DH. Fas/Fas Ligand Interaction in Human Colorectal Hepatic Metastases: A mechanism of hepatocyte destruction to facilitate local tumor invasion. Am J Pathol 1999;154(3):693-703.

18. Müschen M, Moers C, Warskulat U, Niederacher D, Betz B, Even J, Lim A, Josien R, Beckmann MW, Häussinger D. CD95 ligand expression in dedifferentiated breast cancer. J Pathol 1999;189(3):378-86.

19. Repp AC, Mayhew ES, Howard K, Alizadeh H, Niederkorn JY. Role of Fas ligand in uveal melanoma-induced liver damage. Graefe's Arch Clin Exp Ophthalmol. 2001;239(10):752–8.

20. Nagashima H, Mori M, Sadanaga N, Mashino K, Yoshikawa Y, Sugimachi K. Expression of Fas ligand in gastric carcinoma relates to lymph node metastasis. Int J Oncol. 2001;18(6):1157-62.

21. Ohta T, Elnemr A, Kitagawa H, Kayahara M, Takamura H, Fujimura T, Nishimura G, Shimizu K, Yi SQ, Miwa K. Fas ligand expression in human pancreatic cancer. Oncol Rep. 2004; 12(4):749-54.

22. Fais S, Overholtzer M. Cell- in-cell phenomena in cancer. Nat Rev Cancer. 2018;18(12):758-66.

23. Nishio M, Miyachi Y, Otani J, Tane S, Omori H, Ueda F, Togashi H, Sasaki T, Mak TW, Nakao K, Fujita Y, Nishina H, Maehama T, Suzuki A. Hippo pathway controls cell adhesion and context-dependent cell competition to influence skin engraftment efficiency. FASEB J 2019;33(4):5548-60.

24. Kohashi K, Mori Y, Narumi R, Kozawa K, Kamasaki T, Ishikawa S, Kajita M, Kobayashi R, Tamori Y, Fujita Y. Sequential oncogenic mutations influence cell competition. Curr Biol. 2021;31(18):3984-95.

25. Thoma CR, Zimmermann M, Agarkova I, Kelm JM, Krek W. 3D cell culture systems modeling tumor growth determinants in cancer target discovery. Adv Drug Deliv Rev. 2014;69-70:29-41.

26. Moreno E, Basler K. dMyc Transforms Cells into Super-Competitors. Cell. 2004;117(1):117-29.

27. Guicciardi ME, Gores GJ. Life and death by death receptors. FASEB J 2009; 23(6):1625–37.

28. Grootjans S, Berghe TV, Vandenabeele P. Initiation and execution mechanisms of necroptosis: an overview. Cell Death Differ. 2017;24(7):1184-95.

29. Watanabe H, Ishibashi K, Mano H, Kitamoto S, Sato N, Hoshiba K, Kato M, Matsuzawa F, Takeuchi Y, Shirai T, Ishikawa S, Morioka Y, Imagawa T, Sakaguchi K, Yonezawa S, Kon S, Fujita Y. Mutant p53-Expressing Cells Undergo Necroptosis via Cell Competition with the Neighboring Normal Epithelial Cells. Cell Rep. 2018;23(13):3721-9.

30. Penzo-Méndez AI, Chen YJ, Li J, Witze ES, Stanger BZ. Spontaneous Cell Competition in Immortalized Mammalian Cell Lines. PLoS One 201522;10(7):e0132437.

31. Parker TM, Gupta K, Palma AM, Yekelchyk M, Fisher PB, Grossman SR, Won KJ, Madan E, Moreno E, Gogna R. Cell competition in intratumoral and tumor microenvironment interactions. EMBO J. 2021;40(17):e107271.

32. Kmieć Z. Cooperation of liver cells in health and disease. Adv Anat Embryol Cell Biol. 2001;161:III-XIII, 1-151.

33. Wagstaff L, Goschorska M, Kozyrska K, Duclos G, Kucinski I, Chessel A, Hampton-O'Neil L, Bradshaw CR, Allen GE, Rawlins EL, Silberzan P, Carazo Salas RE, Piddini E. Mechanical cell competition kills cells via induction of lethal p53 levels. Nat Commun. 2016;7:11373.

34. Kajita M, Sugimura K, Ohoka A, Burden J, Suganuma H, Ikegawa M, Shimada T, Kitamura T, Shindoh M, Ishikawa S, Yamamoto S, Saitoh S, Yako Y, Takahashi R, Okajima T, Kikuta J, Maijima Y, Ishii M, Tada M, Fujita Y. Filamin acts as a key regulator in epithelial defence against transformed cells. Nat Commun. 2014;5:4428.

35. Chiba T, Ishihara E, Miyamura N, Narumi R, Kajita M, Fujita Y, Suzuki A, Ogawa Y, Nishina H. MDCK cells expressing constitutively active Yes-associated protein (YAP) undergo apical extrusion depending on neighboring cell status. Sci Rep. 2016;6:28383.

36. Baker NE. Emerging mechanisms of cell competition. Nat Rev Genet. 2020;21(11):683-697.

37. Morata G, Ripoll P. Minutes: mutants of drosophila autonomously affecting cell division rate. Dev Biol. 1975;42(2):211-21.

38. Rhiner C, López-Gay JM, Soldini D, Casas-Tinto S, Martín FA, Lombardía L, Moreno E. Flower forms an extracellular code that reveals the fitness of a cell to its neighbors in Drosophila. Dev Cell. 2010;18(6):985-98.

39. Vincent, J. P., Kolahgar, G., Gagliardi, M. & Piddini, E. Steep differences in wingless signaling trigger Myc- independent competitive cell interactions. Dev. Cell 2011;21(2):366–74.

40. van Neerven SM, de Groot NE, Nijman LE, Scicluna BP, van Driel MS, Lecca MC, Warmerdam DO, Kakkar V, Moreno LF, Vieira Braga FA, Sanches DR, Ramesh P, Ten Hoorn S, Aelvoet AS, van Boxel MF, Koens L, Krawczyk PM, Koster J, Dekker E, Medema JP, Winton DJ, Bijlsma MF, Morrissey E, Léveillé N, Vermeulen L. Apc-mutant cells act as supercompetitors in intestinal tumour initiation. Nature. 2021;594(7863):436-441.

41. Flanagan DJ, Pentinmikko N, Luopajärvi K, Willis NJ, Gilroy K, Raven AP, Mcgarry L, Englund JI, Webb AT, Scharaw S, Nasreddin N, Hodder MC, Ridgway RA, Minnee E, Sphyris N, Gilchrist E, Najumudeen AK, Romagnolo B, Perret C, Williams AC, Clevers H, Nummela P, Lähde M, Alitalo K, Hietakangas V, Hedley A, Clark W, Nixon C, Kirschner K, Jones EY, Ristimäki A, Leedham SJ, Fish PV, Vincent JP, Katajisto P, Sansom OJ. NOTUM from Apc-mutant cells biases clonal competition to initiate cancer. Nature. 2021;594(7863):430-435.

42. Moreno E, Basler K, Morata G. Cells compete for decapentaplegic survival factor to prevent apoptosis in Drosophila wing development. Nature. 2002;416(6882):755-9.

43. Martins VC, Busch K, Juraeva D, Blum C, Ludwig C, Rasche V, Lasitschka F, Mastitsky SE, Brors B, Hielscher T, Fehling HJ, Rodewald HR. Cell competition is a tumour suppressor mechanism in the thymus. Nature. 2014;509(7501):465-70.

44. Chi Y, Remsik J, Kiseliovas V, Derderian C, Sener U, Alghader M, Saadeh F, Nikishina K, Bale T, Iacobuzio-Donahue C, Thomas T, Pe'er D, Mazutis L, Boire A. Cancer cells deploy lipocalin-2 to collect limiting iron in leptomeningeal metastasis. Science. 2020;369(6501):276-282.

45. Brás-Pereira C, Moreno E. Mechanical cell competition. Curr Opin Cell Biol. 2018;51:15-21.

46. Thielicke W, Sonntag R. Particle Image Velocimetry for MATLAB: Accuracy and enhanced algorithms in PIVlab. J Open Res Softw. 2021;9(1):12.

47. Moreno E, Valon L, Levillayer F, Levayer R. Competition for Space Induces Cell Elimination through Compaction-Driven ERK Downregulation. Curr Biol. 2019;29(1):23-34.e8.

48. Igaki T, Pastor-Pareja JC, Aonuma H, Miura M, Xu T. Intrinsic tumor suppression and epithelial maintenance by endocytic activation of Eiger/TNF signaling in Drosophila. Dev Cell. 2009;16(3):458-65.

49. Yamamoto M, Ohsawa S, Kunimasa K, Igaki T. The ligand Sas and its receptor PTP10D drive tumour-suppressive cell competition. Nature. 2017;542(7640):246-250.

50. Merino MM, Rhiner C, Lopez-Gay JM, Buechel D, Hauert B, Moreno E. Elimination of unfit cells maintains tissue health and prolongs lifespan. Cell. 2015;160(3):461-76.

51. Krishnakumar S, Kandalam M, Mohan A, Iyer A, Venkatesan N, Biswas J, Shanmugam MP. Expression of Fas ligand in retinoblastoma. Cancer. 2004;101(7):1672-6.

52. Zheng HC, Sun JM, Wei ZL, Yang XF, Zhang YC, Xin Y. Expression of Fas ligand and caspase-3 contributes to formation of immune escape in gastric cancer. World J Gastroenterol. 2003;9(7):1415-20.

53. Bennett MW, O'connell J, O'sullivan GC, Roche D, Brady C, Kelly J, Collins JK, Shanahan F. Expression of Fas ligand by human gastric adenocarcinomas: a potential mechanism of immune escape in stomach cancer. Gut 1999;44(2):156-62.

54. Ibrahim R, Frederickson H, Parr A, Ward Y, Moncur J, Khleif SN. Expression of FasL in squamous cell carcinomas of the cervix and cervical intraepithelial neoplasia and its role in tumor escape mechanism. Cancer. 2006;106(5):1065-77.

55. Fokkema E, Timens W, de Vries EG, de Jong S, Fidler V, Meijer C, Groen HJ. Expression and prognostic implications of apoptosis-related proteins in locally unresectable non-small cell lung cancers. Lung Cancer. 2006;52(2):241-7.

56. Lin Y, Liu L, Zhang T, Liu J. Functional Investigation of Fas Ligand Expressions in Human Non-Small Cell Lung Cancer Cells and Its Clinical Implications. Ann Thorac Surg. 2013;95(2):412-8.

57. Mottolese M, Buglioni S, Bracalenti C, Cardarelli MA, Ciabocco L, Giannarelli D, Botti C, Natali PG, Concetti A, Venanzi FM. Prognostic relevance of altered Fas (CD95)-system in human breast cancer. Int J Cancer. 2000;89(2):127-32.

58. Baldini E, Ulisse S, Marchioni E, Di Benedetto A, Giovannetti G, Petrangeli E, Sentinelli S, Donnorso RP, Reale MG, Mottolese M, Gandini L, Lenzi A, D'Armiento M. Expression of Fas and Fas ligand in human testicular germ cell tumours. Int J Androl. 2009;32(2):123-30.

59. Gutierrez LS, Eliza M, Niven-Fairchild T, Naftolin F, Mor G. The Fas/Fas-ligand system: a mechanism for immune evasion in human breast carcinomas. Breast Cancer Res Treat. 1999;54(3):245-53.

60. Munakata S, Enomoto T, Tsujimoto M, Otsuki Y, Miwa H, Kanno H, Aozasa K. Expressions of Fas ligand and other apoptosis-related genes and their prognostic significance in epithelial ovarian neoplasms. Br J Cancer. 2000;82(8):1446-52.

61. Shimoyama M, Kanda T, Liu L, Koyama Y, Suda T, Sakai Y, Hatakeyama K. Expression of Fas ligand is an early event in colorectal carcinogenesis. J Surg Oncol. 2001;76(1):63-8.

62. Belluco C, Esposito G, Bertorelle R, Alaggio R, Giacomelli L, Bianchi LC, Nitti D, Lise M. Fas ligand is up-regulated during the colorectal adenoma-carcinoma sequence. Eur J Surg Oncol. 2002;28(2):120-5.

63. Bennett MW, O'Connell J, Houston A, Kelly J, O'Sullivan GC, Collins JK, Shanahan F. Fas ligand upregulation is an early event in colonic carcinogenesis. J Clin Pathol. 2001;54(8):598-604.

64. Satchell AC, Barnetson RS, Halliday GM. Increased Fas ligand expression by T cells and tumour cells in the progression of actinic keratosis to squamous cell carcinoma. Br J Dermatol. 2004;151(1):42-9.

65. Nozoe T, Yasuda M, Honda M, Inutsuka S, Korenaga D. Fas ligand expression is correlated with metastasis in colorectal carcinoma. Oncology. 2003;65(1):83-8.

66. Kykalos S, Mathaiou S, Karayiannakis AJ, Patsouras D, Lambropoulou M, Simopoulos C. Tissue expression of the proteins fas and fas ligand in colorectal cancer and liver metastases. J Gastrointest Cancer. 2012;43(2):224-8.

67. Pernick NL, Sarkar FH, Tabaczka P, Kotcher G, Frank J, Adsay NV. Fas and Fas ligand expression in pancreatic adenocarcinoma. Pancreas. 2002;25(3):e36-41.

68. Lee WC, Yu MC, Chen MF. Prognostic impact of Fas ligand on hepatocellular carcinoma after hepatectomy. World J Surg. 2004;28(8):792-6.

69. Kase H, Aoki Y, Tanaka K. Fas ligand expression in cervical adenocarcinoma: relevance to lymph node metastasis and tumor progression. Gynecol Oncol. 2003;90(1):70-4.

70. Munakata S, Watanabe O, Ohashi K, Morino H. Expression of Fas ligand and bcl-2 in cervical carcinoma and their prognostic significance. Am J Clin Pathol. 2005;123(6):879-85.

71. Igney FH, Behrens CK, Krammer PH. Tumor counterattack--concept and reality. Eur J Immunol. 2000;30(3):725-31.

72. Houston A, O'Connell J. The Fas signalling pathway and its role in the pathogenesis of cancer. Curr Opin Pharmacol. 2004;4(4):321-6.

73. Igney FH, Krammer PH. Tumor counterattack: fact or fiction? Cancer Immunol Immunother. 2005;54(11):1127-36.

74. Grimm M, Gasser M, Bueter M, Strehl J, Wang J, Nichiporuk E, Meyer D, Germer CT, Waaga-Gasser AM, Thalheimer A. Evaluation of immunological escape mechanisms in a mouse model of colorectal liver metastases. BMC Cancer. 2010;10:82.

75. Hoglen NC, Chen LS, Fisher CD, Hirakawa BP, Groessl T, Contreras PC. Characterization of IDN-6556 (3-[2-(2-tert-butyl-phenylaminooxalyl)-

amino]-propionylamino]-4-oxo-5-(2,3,5,6-tetrafluoro-phenoxy)-pentanoic acid): a liver-targeted caspase inhibitor. J Pharmacol Exp Ther. 2004;309(2):634-40.

76. Clavería C, Giovinazzo G, Sierra R, Torres M. Myc-driven endogenous cell competition in the early mammalian embryo. Nature. 2013;500(7460):39-44.

77. Brás-Pereira C, Moreno E. Mechanical cell competition. Curr Opin Cell Biol. 2018;51:15-21.

78. Sun Q, Luo T, Ren Y, Florey O, Shirasawa S, Sasazuki T, Robinson DN, Overholtzer M. Competition between human cells by entosis. Cell Res. 2014;24(11):1299-310.

79. Hamann JC, Surcel A, Chen R, Teragawa C, Albeck JG, Robinson DN, Overholtzer M. Entosis Is Induced by Glucose Starvation. Cell Rep. 2017;20(1):201-210.

80. Levayer R. Solid stress, competition for space and cancer: The opposing roles of mechanical cell competition in tumour initiation and growth. Semin Cancer Biol. 2020;63:69-80.

81. Basan M, Risler T, Joanny JF, Sastre-Garau X, Prost J. Homeostatic competition drives tumor growth and metastasis nucleation. HFSP J. 2009;3(4):265-72.

82. Helmlinger G, Netti PA, Lichtenbeld HC, Melder RJ, Jain RK. Solid stress inhibits the growth of multicellular tumor spheroids. Nat Biotechnol. 1997;15(8):778-83.

83. Montel F, Delarue M, Elgeti J, Malaquin L, Basan M, Risler T, Cabane B, Vignjevic D, Prost J, Cappello G, Joanny JF. Stress clamp experiments on multicellular tumor spheroids. Phys Rev Lett. 2011;107(18):188102.